References

[1] R.B. Singh, S. Mahanta, S. Kar and N. Guchhait, *J. Lumin.* 128 (2008) 1421-1430.

[2] N. Dash, F.A.S. Chipem, R. Swaminathan and G. Krishnamoorthy, *Chem. Phys*. 460 (2008) 119-124.

[3] Z. R. Grobawski, *Pure & Appl. Chem.* Vol. 65, No.8, (1993), 1751-1756.

[4] S.Sumalekshmy and K.R. Gopidas, *J.Phys. Chem. B* 2004,108,3705-3712

[5] R.B. Singh, S.Mahanta, S Kar and N. Guchhait, *Chem Phys.* 342 (2007)33-42

[6] A. Kawski, B. Kuklinski and P. Bojarski, *Chem. Phys.* 455 (2008) 52-54.

[7] R.Daum, S. Druzhinin, D. Earnst, L.Rupp, J.Schroeder, K.A. Zachariasse, *Chem. Phys. Letters* ,

[8] M.Balon, C. Carmona, M.A. Munoz, *Chem. Phys.* 302, 2004.

[9] C. Yao, H. B. Kraatz, R. Steer, *Photochem. Photobiol.Sci*, 4, 2005,191-199

[10] P. Purkayastha, N. Chattopadhyay, *Phys. Chem. Chem. Phys*, 2000, 2, 203-210

[11] A.M.J. Campana, F.A. Barrero, M.R. Ceba, Analyst, 1992, 117

[12] M. Kagayama, Y. Sasano, H. Satos, S. Kamakura, K. Motegi, I.M. Izoguchi, *J. Anathomy and Embryology*, 2004, 233-238

[13] A. Polimeno, A. Barbon, P.L. Nordio, *J.Phys. Chem.* 98, 12158-12168

[14] A. Maliakal, G. Lem, N.J. Turro, R. Ravichandran, J.C. Suhadolink, A.D. Debellis, M.G. Wood, J. Lau, *J.Phys. Chem. A* 2004, 106, 2002, 7680-7689

[15] I. Szydlowska, A. Kyrychenko, A. Gorski, J. Waluk, J. Herbich, *Photochem. Photobiol.Sci*, 2, 2003, 187-194

[16] J. Dobkowski, W. Retting, J. Waluk, *Phys. Chem. Chem. Phys*, 4,2002, 4334-4339

[17] R.B. Singh, S. Mahanta, S. Kar and N. Guchhait, *J. Lumin.* 128 (2008) 1421-1430.

[18] T. Pal, M. Paul and S. Ghosh, *J. Mol. Struct. (THEOCHEM)* 860 (2008) 8-12

[19] J. D. Walson, *Prac. Nat. Acad. Sci, USA*, 69,9,1972, 2488-2491

[20] S. Maheshwari, A. Chowdhury, N. Sathyamurthy, M. Panda, J. Chandrasekhar, *J.Phys. Chem. A*,103, 1999, 6257-6262

[21] T.L. Arbeloa, F.L. Arbeloa, M.J. Tapia, I.L. Arbeloa, *J.Phys. Chem.* 97, 1993, 4704-4707

[22] Z.R. Grabowski, Pure & Applied Chem, 65,8, 1993, 1751-1756

[23] F. Pine, M.J. Melo, H. Santos, J.C. Lima, I. Abreu, R. Ballardini, M. Maestri, New J. Chem., 1998, 1093-1098

[24] C. Richardit, Solvent and Solvent effect in organic chemistry, 3rd edition, WILLEY-VCH, Weinheim, 2003, 329-387.

[25] Dobkowski J., Wojcik J., Kozminski W., Kols R., Waluk J., Michl J.; *J. Am. Chem. Soc.* 2002, 124, 2406.

[26] Yoshihara T., Druzhinin S. I., Zachariasse K., *J. Am. Chem. Soc.* 2004, 126, 8535.

[27] Okamoto H., Inishi H., Nakamura Y., Kohtani S., Nakagaki R., *J. Phys. Chem. A* 2001, 105, 4182-4188.

[28] Kowk W. M., Matousek P., Parker A. W., Phillips D., Toner W. T., Towrie M., Umapathy S., *J. Phys. Chem. A* 2001, 105, 984-990.

[29] Dreyer J., Kummrow A. *J. Am. Chem. Soc.* 2000, 122, 2577-2585.

[30] Zilberg, S.; Haas, Y. *J. Phys. Chem. A* **2002**, *106*, 1-11.

[31] Rappoport, D.; Furche, F. *J. Am. Chem. Soc.* **2004**, *126*, 1277-1284.

[32] Köhn, A.; Hättig, C. *J. Am. Chem. Soc.* **2004**, *126*, 7399-7410.

[33] Serrano-Andrés, L.; Merchán, M.; Roos, B. O.; Lindh, R. *J. Am. Chem. Soc.* **1995**, *117*, 3189-3204.

[34] Sobolewski, A. L.; Sudholt, W.; Domcke, W. *J. Phys. Chem. A* **1998**, *102*, 2716-2722.

[35] Parusel, A. B. J.; Köhler, G.; Grimme, S. *J. Phys. Chem. A* **1998**, *102*, 6297-6306.

[36] Parusel, A. B. J.; Köhler, G.; Nooijen, M. *J. Phys. Chem. A* **1999**, *103*, 4056-4064.

[37] Kim, H. J.; Hynes, J. T. *J. Photochem. Photobiol., A: Chem.* **1997**, *105*, 337-343.

[38] Mennucci, B.; Toniolo, A.; Tomasi, J. *J. Am. Chem. Soc.* **2000**, *122*, 10621-10630.

[39] Semyon Cogan, Shmuel Zilberg, and Yehuda Haas, *J. Am. Chem. Soc.* **2006**, 128, 3335-3345.

[40] M. Barzoukas, C. Runser, A. Fort, M. Blanchard-Desce, *Chem. Phys. Letters* , 257, 1996, 531-537.

[41] F. Wurthner, S.Yao, J. Schilling, R. Wortmann, M. Redi-Abshiro, E. Mecher, F. Gallego-Gomez, K. Meerhlz

[42] A.Yu, Catherine A., D.A. Farrow, D.M Jonas, *Phys. Chem. A* **2002,** 106, 9407-9419

[43] Frank Jensen, *Introduction to computational chemistry*, WILEY, 2004,

ADDIS ABABA UNIVERSITY

SCHOOL OF GRADUATE STUDIES

DEPARTMENT OF CHEMISTRY

Investigation of Excitation Wavelength and Solvent Polarity Dependence of Dual Fluorescence of a Newly Synthesized Schiff Base,

N-(4-(dimethylamino) benzylidene)-2H-1, 2, 4-triazol-3-amine (DMABA-Amtr)

Advisor: Dr. Mesfin Redi

By

Ephriem Tadesse

A project submitted to the School of Graduate Studies in partial fulfillment of the requirement for the Degree of Master of Science in Chemistry

Addis Ababa

Jul, 2009

Acknowledgement

I would like to express my deepest gratitude and appreciation to my advisor, Dr. Mesfin Redi, for his day to day follow up, genuine advices, comments and devoted supports and encouragement during the entire period of this project and through my seminar works. It is intellectually stimulating, rewarding and priceless experience to work with him. It is truly an honor and a privilege to work with him.

I would like to thank also Mr. Belina for all his supports, guidance and encouragement. He is really a good person to work with.

I also thank all my professors for their valuable inputs during my study.

I am also grateful to thank all my friends and families who are always there for me.

My special thanks go to Haramaya University for the financial support.

Abstract

Steady state absorption, fluorescence excitation and emission spectra of DMABA-Amtr have been measured at room temperature in cyclohexane (CHEX), 1,4-dioxane (DOX), dichloromethane (DCM), acetonitrile (ACN) and hexanol solutions. The compound is found to exhibit dual emission in polar solvents while a single emission was observed in a nonpolar solvent cyclohexane. The effect of solvent polarity on the absorption spectra shows a general bathochromic shift. Dependence of the emission spectra on solvent polarity and excitation wavelength has also been studied. The fluorescence excitation spectra of DMABA-Amtr monitored at different emission bands are found to be different. Moreover, area normalized emission spectra in polar solvents exhibit an isoemissive point showing the presence of two equilibrated ground state conformations of the same molecule. Thus, the presence of two different conformations of the same molecule in the ground state in polar solvents has led to two wxcited states, locally excited (LE) and charge transfer (CT), and thereby results in the dual fluorescence of the compound.

The experimental studies were supported by computational results, force field theory/ Molecular Mechanics/ MM^{+}, by making use of Hyperchem 7.5 software. The ground state geometry optimization and value of the ground state dipole moment was computed at Density Functional Theory (DFT) level with B3LYP functional and 6-31G basis set.

On the basis of the experimental and computational results, two conformers of DMABA-Amtr are suggested which are stable in the ground state, equilibrated in polar solvents at room temperature that give rise to dual fluorescence up on excitation.

Declaration

This project is my original work, has not been presented in this or other University and that all resources and materials used for this project have been duly acknowledged.

Name: Ephriem Tadesse

Signature: _____

The project has been submitted for examination with our approval as university advisor

Declaration

I the undersigned confirm that the results reported in this work were obtained by research carried out by myself under the supervision of mu advisor in the Faculty of Science, Department of Chemistry, Addis Ababa University in the academic year 2008/09. No part of this work shall be published in scientific journals or reported in the media or presented at a conference without the knowledge and consent of my advisor, who is the principal scientist responsible for any publication.

Name: Ephriem Tadesse Signature _____

This Project work has been submitted for examination with my approval as a university advisor.

Advisor: Dr. Mesfin Redi Signature _____

Place and date of submission: School of Graduate Studies, Addis Ababa University

July, 2009.

ADDIS ABABA UNIVERSITY

SCHOOL OF GRADUATE STUDIES

DEPARTMENT OF CHEMISTRY

Investigation of Excitation Wavelength and Solvent Polarity Dependence of Dual Fluorescence of a Newly Synthesized Schiff Base,

N-(4-(dimethylamino) benzylidene)-2H-1, 2, 4-triazol-3-amine (DMABA-Amtr)

Advisor: Dr. Mesfin Redi

By

Ephriem Tadesse

Approved by the examining board :-

	Date	Signature
Dr. Mesfin Redi (Advisor)	_____	_____
Dr. Shimelis Admassie (Examiner)	_____	_____
Dr. Ahmed Mustefa (Examiner)	_____	_____

Table of contents

1. Introduction

The basic process involved in the excited state intramolecular charge transfer (ICT) reactions is an interesting arena for researchers in the field of physical chemistry and chemical physics. Even after decades of the discovery of dual fluorescence in 4-*N*,*N*-dimethylaminobenzonitrile (DMABN) by Lippert et. al, new molecules are being designed for the possibility of Photo induced ICT reaction. The need for new donor-acceptor charge transfer (CT) molecules crops up due to their vast application in the field of pure and applied sciences such as pH and ion detectors, sensors, study of micro heterogeneous environment etc. The need multiplied when it became clear that Photo induced ICT may play a crucial role in biological light harvesting processes such as photosynthesis and vision [1].

Bichromophoric organic molecules composed of directly attached electron donor and electron acceptor moieties have received considerable attention as possible models for a number of photochemical and photo biological processes. Excitation of such molecules induces transfer of an electron from donor to acceptor and is often accompanied by rotational relaxation to a twisted conformation of the donor relative to the acceptor, forming the so called Twisted Intramolecular Charge Transfer (TICT) state [2,3].

Molecules of the type $D-\pi-A$ where the donor and acceptor groups are connected to the ends of a conjugated system exhibit large changes in dipole moment ($\Delta\mu$) up on excitation due to photoinduced Intramolecular charge transfer process. The extent of charge transfer depends on the nature of the donor (D) and acceptor (A) groups and the length of the π system. Conformational dynamics of the D and A fragments can also significantly influence the photochemistry of such systems. Lengthening of the π-system in D-π-A is expected to increase the $\Delta\mu$ term, resulting in substantial red-shift of the fluorescence spectrum [4].

Over the past years, the photophysical study of $D-\pi-A$ systems linked to a chromophore has drawn considerable interest for basic and applied research. The first observation of dual fluorescence of the benchmark molecule 4-*N*,*N*'-dimethylaminobenzonitrile (DMABN) by Lippert et al. was a major breakthrough in the realm of photo induced D-π-A charge transfer process. Since then, spectroscopic study in combination with high level quantum chemical calculations have been devoted for the investigation of charge transfer reaction in a variety of $D-\pi-A$ systems [5].

Since the discovery of dual emission of DMABN in fluid solvents of high polarity, numerous polar organic compounds demonstrate dual fluorescence. In non-polar solvents, only a short wavelength emission band appears [6].

The origin of dual fluorescence of DMABN and related compounds in solutions continues to be the subject of detailed investigation and controversial discussion [7]. In the study of dual luminescence phenomena significant attention has been paid to the donor acceptor substituted aromatics which are best represented by DMABN, 4-*N*,*N*'-dimethylaminobenzaldehyde (DMABA) and related compounds [8-12].

Almost all the studies so far are concerned with the excited state structural rearrangements, and thus do not give insight about the possible ground state ground state origin of the dual fluorescence. Unlike the earlier reported studies, emphasis is given for the ground state phenomena.

In this work, dual fluorescence is obtained for a newly synthesized molecule, DMABA-Amtr in polar solutions. The effect of polar solvents on the excitation and emission spectra of DMABA-Amtr is studied. In addition the effect of polar solvents on the absorption spectra, ground state structure and related consequences on dual fluorescence properties of the compound are investigated both experimentally and computationally.

2. Mechanism of Dual Fluorescence

In general, single excitation bands possess a single fluorescence band. There are cases, however, where two fluorescence bands are observed in compounds even in the case of simple donor-acceptor substituted benzene, DMABN. The first band around 350 nm corresponds to the "normal" band for closely related benzene derivatives and the other one at considerably longer wavelength was assigned to an "anomalous" band [13]. The anomalous band was assigned to fluorescence from the more polar ^1L_a-type state which is preferentially stabilized by solvation. This has led to the nomenclature in photophysics 'A' band for the "anomalous" emission from the ^1L_a-type state or charge transfer state and 'B' band for the "normal" short wavelength emission from the ^1L_b-type state or locally excited (LE) state.

It has been discovered that dual fluorescence depends strongly on solvent polarity and temperature [14]. In non-polar solvents, DMABN and related compounds were found to exhibit

normal emission related to the benzene derivatives around $\lambda_{max} = 350\,nm$. However, in polar environment, in addition to the normal fluorescence, an "anomalous" red-shifted band was observed. It was solvent polarity dependent with λ_{max} from 420 nm to 500 nm [15]. This band was called "anomalous" because it constituted an obvious exception from the Kasha rule stating 'the fluorescence spectrum is dominated by a single band arising from emission from the first excited singlet state'. These fluorescence bands were assigned to emission from the close lying ^1L_a and ^1L_b states. In non-polar solvents, the ^1L_b- state is lower in energy than the ^1L_a-state and hence only the 'B' band is observed. On the other hand, in polar-solvents, the ^1L_a- state involving greater charge transfer is lowered due to the interaction of the dipole moments of the excited state species and solvent molecules; hence 'A' band fluorescence is observed [16].

Different hypotheses were formulated to interpret dual fluorescence. These are emissions from an excimer, proton transfer, hydrogen bonding, and formation of exciplex with the solvent, Twisted Intramolecular Charge Transfer (TICT), Wagging of the amino group (WICT), Rehybridization of the acceptor (RICT) and planarization of the molecule (PICT). However, many of the hypotheses are being discarded by ample experimental and theoretical results. The two main hypotheses which still stand and go with most of the theoretical and experimental evidences are the TICT and PICT models [1, 4-12, 17].

The implicit assumption of the TICT model, which was first put forward by Grabowski et al and co-workers in 1970's, is the twisting motion of the donor group and latter refined as a 90^0 twisted conformation of the $-NMe_2$ (donor) group in the ICT state. This twisting takes the initially generated locally excited state to another energy minimum on the excited state potential energy surface (PES). In DMABN, DMABA and related compounds, the concept of TICT stated that in the twisted conformation of the donor $-NMe_2$ group is twisted 90^0 out of the plane of the benzene moiety and hence completely decoupled from the acceptor group. Under this condition, a complete charge transfer takes place and the ^1L_a-band is thought to be responsible for the charge transfer emission from this twisted conformer [18-20]. The process of TICT is summarized in Figs.1 and 2.

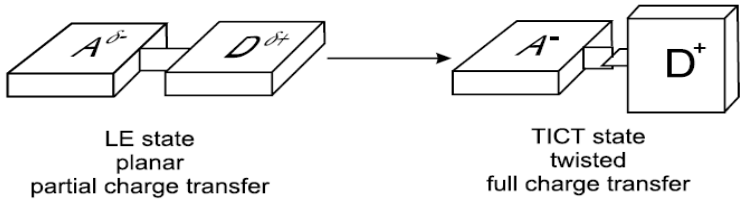

Fig. 1 TICT model for donor-acceptor system (Taken from Ref. 44)

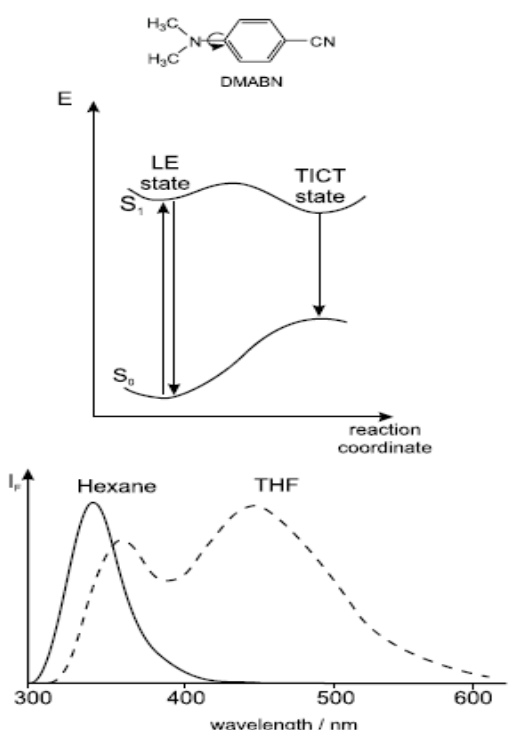

Fig. 2 Potential energy diagram of DMABN (top); the reaction coordinate contains both solvent relaxation and rotation of the dimethylamino group. Room temperature fluorescence spectrum in hexane and tetrahydrofurane, THF (bottom). (Taken from Ref.44)

On the other hand, the so called planar ICT (PICT) model was advocated by Zachariasse and co-workers in series of papers since 1993 [21, 22]. The basic assumption of this model is that, in the ICT state, the donor and acceptor groups are not decoupled and that the configuration change of the amino nitrogen from the pyramidal towards planar is an important reaction coordinates. In the PICT model, independent of the structure of the ICT state, a small energy gap ΔE between the two lowest excited singlet states is considered to be an important requirement for the occurrence of dual fluorescence [23, 24]. Experimental evidence advanced for both models has been largely circumstantial, as direct measurement of the structure of the emitting species turns out to be experimentally difficult. Nonetheless, equally convincing indirect evidence has been presented for the TICT and PICT models. For instance, by a suitable construction, Dobrowski et al. [25] showed that the CT process is accompanied by syn-anti isomerization around the C-phenyl-N bond in the photoisomerization of 2-(N-methyl-N-isopropylamino)-5-

cyanopyridine, a process that implies the intermediacy of a perpendicular moiety. On the other hand, Yoshihara et al. [26] showed that a planarized molecule that cannot attain a perpendicular geometry exhibits dual emission. The planar rigidized molecule fluorazene (FPP) was shown to undergo fast reversible intramolecular charge transfer (ICT) in the excited state, similar to that of its flexible counterpart N-phenylpyrrole (PP). This result shows that intramolecular charge transfer to a planar ICT state can occur efficiently and thus convincingly demonstrates that large amplitude motions such as those necessary for the formation of a TICT state are not required.

Experimentally, from picosecond infrared [27] and resonance Raman [28] measurements, and calculations of IR frequencies [29], it was concluded that the N-phenyl bond has a single-bond character in the ICT state, which would support the TICT model. Theoretical computations [30] suggest that the ICT state has a strong quinoidal character in the phenyl moiety (which would favor the PICT structure), and a decrease of quinoidality would be expected when the amino group was decoupled from the rest of the molecule in TICT. In their calculations, Zilberg and Haas [30] could only find a planar quinoid ICT state on the S_2 surface of ABN and no quinoidal TICT structure. However, several calculations [29, 31, 32] have found a quinoidal TICT state on S_1, including the most recent correlated CC2 (coupled-cluster singles and doubles) calculations by Köhn [32]. Thus, the twisted conformation of the amino group and the quinoidality of the phenyl ring may not be as contradictory as first thought.

Theoretical contributions have also given some insight as to the nature of the ICT reaction coordinate. As a general rule, most theoretical studies point toward the amino group twist as the reaction coordinate along which a state switch occurs (either at conical intersection or at an avoided crossing giving rise to a transition state) between the LE and ICT states and leads to a low-lying TICT state [33-38]. However, recent high level *ab-initio* calculations have suggested that those two states can cross along the pyramidalization of the ring carbon atom to which the dimethylamino group is attached, without the twisting motion. Thus, this pyramidalization coordinate constitutes another possible decay path after initial vertical excitation to the L_a-type state.

More recently, Cogan et al. [39] pointed out that the benzene ring was not acting merely as a spacer between the donor and the acceptor but is essential for understanding the electronic structure of the excited states. This idea that the benzene ring is the principal electron acceptor leads naturally to the four distinct lowest lying electronic excited states in these systems: two are

principally of LE nature, whereas the other two are CT-types. It is shown that both planar and twisted forms of the molecule in the CT state may be fluorescent, depending on the structure of the system and on environmental parameters such as the solvent. Further, their model predicts also the existence of a perpendicular quinoid (Q)-form having a large dipole moment. The emitting charge transfer state is due to the transfer of an electron from the donor group to the benzene ring, creating a derivative of the benzene anion radical. Two electronic states are necessarily formed as a consequence of the Jahn-Teller distortion of the benzene anion radical: one has a quinoid structure, the other, an antiquinoid one. The model provides a simple explanation for the direct excitation of the CT states (i.e. not via the LE state) observed in supersonic jets and in argon matrixes.

The desire to uncover the reason for unique chemical properties of DMABN, DMABA and related compounds has triggered a large number of experimental and theoretical studies, and many reviews exist. Nevertheless, even for DMABN, the well studied molecule, the mechanism of ICT reaction is still a matter of controversial debate.

So far, the theoretical models proposed have been exclusively focusing on the excited state structural arrangements giving little or no consideration on the ground state possible structural isomers. In this work, the excitation wavelength dependence of dual fluorescence of DMABA-Amtr in different solvents is investigated. The dual fluorescence of DMABA-Amtr is assessed in those solvents from the perspective of ground state structural isomeric structures. Moreover, computational calculations are employed for qualitative understanding of its photophysical properties.

3. Theory of Solvatochromic Shifts

When absorption spectra are measured in solvents of different polarity, it is found that these solvents usually modify the position, intensities and shapes of the absorption bands. These changes are results of physical intermolecular solute-solvent interaction forces (such as ion-dipole, dipole-dipole, dipole-induced dipole, hydrogen bonding etc.), which above all tend to alter the energy differences between ground and excited state of the absorbing species containing the chromophore. The medium influence on absorption spectra can be considered comparing the spectral changes observed (i) on going from the gas phase to solution or (ii) simply by changing

the nature of the solvent. Because of the difficulty in measuring the absorption spectrum in the gas phase, the second method is applied in most cases.

Theories of solvent effects on absorption spectra assume principally that the chemical state of the isolated and solvated chromophore containing molecule are the same and treat these effects only as a physical perturbation of the relevant molecular state of the chromophores. These solvent effects on absorption spectra can be used to provide information about solute-solvent interactions.

The term solvatochromism is used to describe the pronounced change in position (and sometimes intensity) of a UV/Vis absorption band that accompanies a change in polarity of the medium. A hypsochromic (or blue) shift with increasing solvent polarity is usually called negative solvatochromism. The corresponding bathochromic (or red) shift is termed positive solvatochromism.

The solvent effect on spectra, resulting from electronic transitions, is primarily dependent on the chromophore and the nature of transition ($\sigma^* \leftarrow \sigma, \sigma^* \leftarrow n, \pi^* \leftarrow \pi, \pi^* \leftarrow n,$ and charge transfer (CT) absorption). The electronic transitions of particular interest in this respect are $\pi^* \leftarrow \pi, \pi^* \leftarrow n$, and charge transfer (CT) absorptions. Organic compounds with chromophores containing π-electrons can be classified in to three different groups according to their idealized π-electronic structure: aromatic compounds, polyenes, and polymethines (Fig. 3) [24]

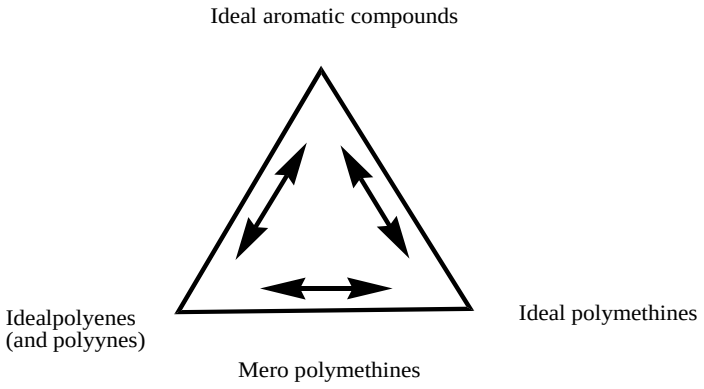

Fig. 3 Classification of organic compounds with π-electron systems according to Dahne.

$(n+3)\pi$ $\quad n = 1,3,5,\ldots$

$X-(CR)_n-X'$ $\quad R = H$ or substituent

$X, X' =$ terminal chain atoms (N, O, S, P) or atom groups

$X = X'$ polymethine dyes ($X = X' = N$: cyanine; $X = X' = O$: oxonols)

$X \neq X'$ meropolymethine dyes ($X = N$ *and* $X' = O$; merocyanines)

A push-pull molecule, containing donor and acceptor groups connected via a π-conjugated path, like DMABA-Amtr exhibit a low lying absorption band in polar solutions. This ground-to-excited state transition, possessing large oscillator strength, is assigned to an electronic intramolecular charge transfer (ICT) between end groups.

A push-pull molecule can be viewed as a mixture between neutral and charge separated (zwitterionic) resonance forms (Fig.4).

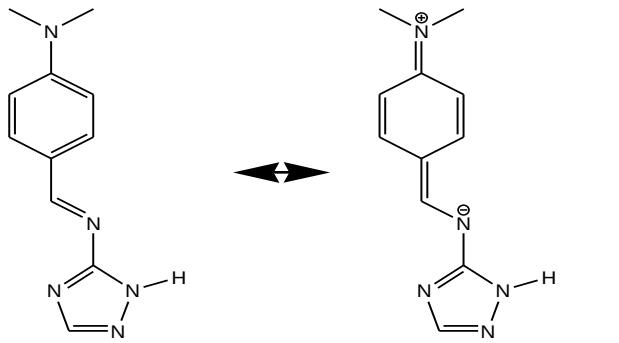

Fig.4 Neutral and Charge separated (zwitterionic) resonance forms of a push pull molecule.

Application of static electric field E of varying magnitude across the molecule can tune the ground state geometry from the "gas phase" structure to the zwitterionic structure. In solution, solvent molecules generate an electric reaction field across a push-pull molecule. Increasing the solvent polarity strengthens the magnitude of this field, so that it can induce more charge separation in the ground state of the push-pull molecule [40].

The electric properties of the dye may also be analyzed in terms of a simple CT model, which describes the ground and excited state as linear combinations of the neutral and zwitterionic resonance structures based on a resonance parameter c^2. Within this crude model, donor-acceptor substituted π-conjugated chain molecules may be classified from polyene-type

($c^2 \approx 0$) over neutrocyanines ("cyanine limit", $c^2 \approx 0.5$) to betaine-type systems ($c^2 \approx 1$). A second parameter of this model is the maximal hypothetical dipole change $\Delta\mu_{max}$, the difference of the dipole moments of the neutral and zwitterionic resonance structure. Since this difference is proportional to the charge separation distance, $\Delta\mu_{max}$ can be regarded as a measure of the effective CT length of the donor-acceptor system. The model parameters c^2 and $\Delta\mu_{max}$ can be determined from the values of the transition dipole moment and the dipole difference

$$c^2 = \frac{1}{2}\left(1 - \Delta\mu(4\mu_{eg}^2 + \Delta\mu^2)^{-1/2}\right) \quad (1)$$

$$\Delta\mu_{max} = \Delta\mu/(1-2c^2) \quad (2)$$

Where μ_{eg} is the transition dipole moment [41].

A qualitative interpretation of solvatochromic shifts is possible by considering (a) the momentary transition dipole moment present during the optical absorption, (b) the difference in permanent dipole moment between the ground and excited state of solute, (c) the change in ground state dipole moment of the solute induced by the solvent and (d) the Franck-Condon principle. According to Bayliss and Mc Rae, four limiting cases can be distinguished for intramolecular electronic transitions in solution [24].

i) Nonpolar solute in a non polar solvent: in this case, only dispersion forces contribute to the solvation of the solute. Dispersion forces, operative in any solution, invariably cause a small bathochromic shift, the magnitude of which is a function of the solvent refractive index n, the transition intensity, and the size of the solute molecule. The function $(n^2-1)/(2n^2+1)$ has been proposed to account for this general red shift.

ii) Nonpolar solute in a polar solvent: in the absence of a solute dipole moment, there is no significant orientation of solvent molecules around the solvent molecules, and again a general red shift, depending on the solvent refractive index n, is expected. Solute quadrupole/solvent dipole interaction also should be taken in to account in this case.

iii) Dipolar solute in nonpolar solvent: the forces contributing to solvation are dipole-induced dipole and dispersion forces. If the solute dipole moment increases during the electronic transition, the Franck-Condon excited state is more solvated by dipole-solvent polarization, and a red shift depending on the solvent refractive index n and the change in the solute dipole moment

is expected. The Franck-Condon excited state is less solvated if the solute dipole moment decreases during the electronic transition, and a blue shift, again proportional to the two above mentioned factors, is expected. In the latter case, the resultant shift may be red or blue depending on the relative magnitude of the red shift caused by polarization and the blue shift.

iv) Dipolar solute in a polar solvent: since the ground state solvation results largely from dipole-dipole forces in this case, there is an oriented solvent cage around the dipolar solute molecule, resulting in the net stabilization of their ground state. If the solute dipole moment increases during the electronic transition ($\mu_g < \mu_e$), the Franck-Condon excited state is formed in a solvent cage of already partly oriented solvent dipoles. The better stabilization of the excited state relative to the ground state with increasing solvent polarity will result in a bathochromic shift. Its magnitude will depend on the extent of the change in the solute dipole moment during the transition, the value of the solvent dipole moment and the extent of interaction between the solute and solvent molecules. This situation is schematically illustrated in Fig.5.

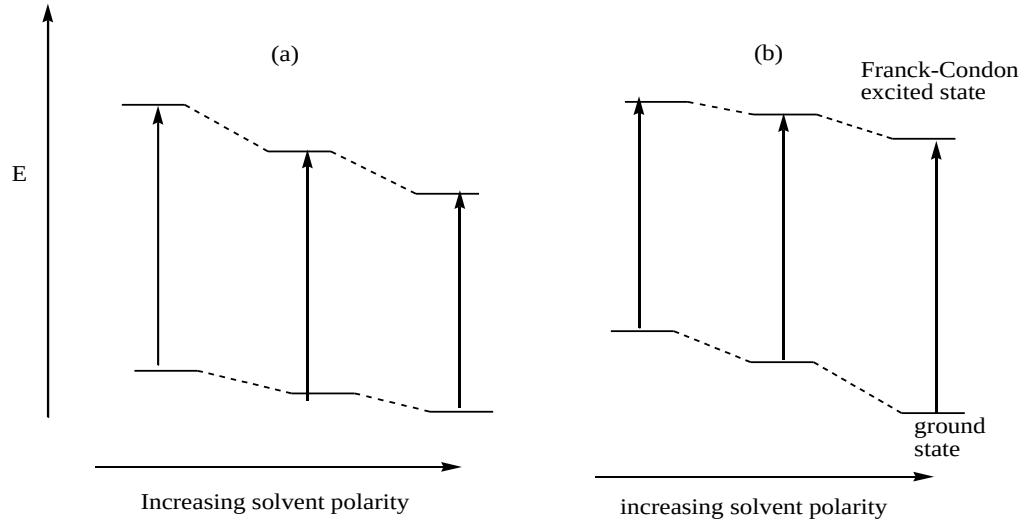

Fig. 5 Schematic qualitative representation of solvent effects on the electronic transition energy of dipolar solute in polar solvent, (a) $\mu_g < \mu_e$; (b) $\mu_g > \mu_e$.

The solvatochromic effect observed is more clearly presented in Fig.6.

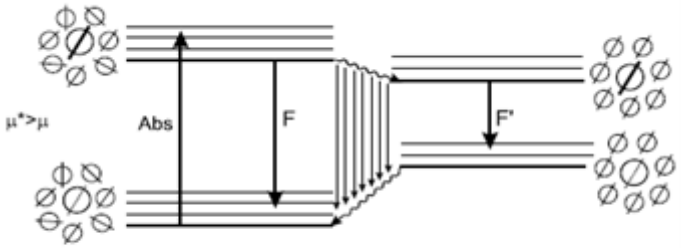

Fig. 6 Solvent relaxation around a probe that has a weak dipole moment in the ground state and large dipole moment in the excited state.

If the dipole moment of the solute decreases during the electronic transition, the Franck-Condon excited state is formed in a strained solvent cage of oriented dipoles not correctly disposed for its efficient stabilization. Thus, with increasing solvent polarity, the energy of the ground state is lowered more than that of the excited state, and this produces a hypsochromic shift.

For a meropolymethine dyes such as the positively solvatochromic merocyanine described below, increasing solvent polarity should shift the electronic structure from a polyene like state (a) to a more polymethine –like state (b) (Fig.7)

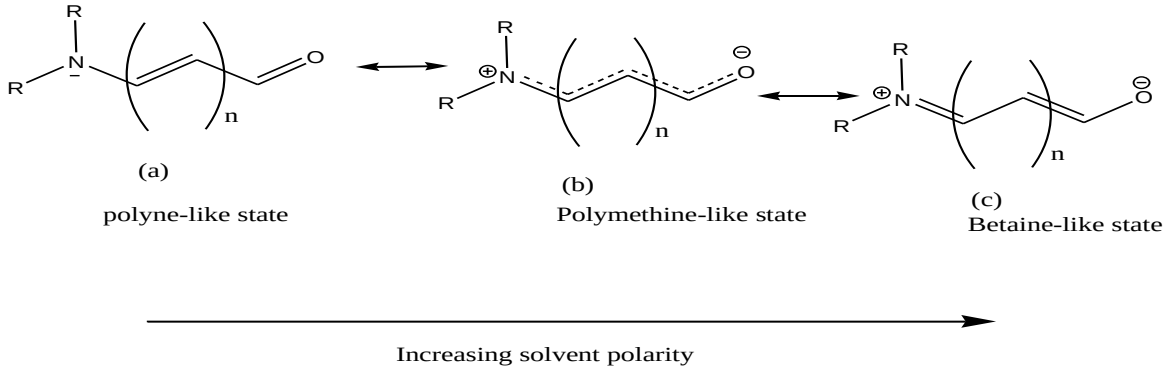

Fig. 7 Polyene (a), Polymethine (b) and Betaine (c) like structures of meropolymethine dyes.

The effect of such a change in electronic ground state structure on the position of the absorption band was calculated by Forster in 1939. According to his calculation, an intermediate meropolymethine (b) with equal contribution of both mesomeric structures (a) and (c) will have the longest wave length absorption. Therefore, a chromophore with a polyene-like electronic structure will exhibit a bathochromic shift with increasing solvent polarity whereas a

chromophore with a polymethine like structure will show a hypsochromic shift on the same solvent cage.

3.1 Quantitative Treatment of Solvatochromic Shift

Since the work of Onsager, various workers have proposed different functions of the dielectric constant, ε and refractive index, n to describe solvatochromism, the solvent dependent shift in absorption and emission spectra [42]. The key idea is that the electrons in the solvent will instantly adapt to a new charge distribution up on electronic excitation, while the nuclear degrees of freedom of the solvent will equilibrate only after the electronic excitation in accord with the Franck-Condon principle. The instantaneous electronic response is reflected in the optical refractive index, while the subsequent nuclear relaxation is reflected in the static dielectric constant. The relative importance of these contributions depends on the solute dipole moment, the solute dipole moment change up on excitation and the change in solute polarizability.

For a polar molecule in a polar solvent, forces orient the solvent to stabilize the polar solute. For a polarizable point dipole in a spherical cavity, the ground state dipole moment, μ_g of the solute induces a solute reaction field, E_g such that

$$E_g = \frac{2(\varepsilon - 1)}{2\varepsilon + 1} \frac{(\mu_g + \alpha E_g)}{a^3} \tag{3}$$

Where ε is the solvent dielectric constant, a is the solute radius, and α is the solute polarizability. Two approaches to solvatochromism diverge from eq.1. The first neglect the solvent polarizability so that the equation becomes

$$E_g = \frac{2\mu_g(\varepsilon - 1)}{a^3(2\varepsilon + 1)} \tag{4}$$

This is appropriate when the reaction field is too weak to appreciably increase the total solute dipole moment. The second approach assumes an approximate relationships between solvent cavity size and solute molecular polarizabilities such as $\alpha = a^3/2$, and the equation becomes

$$E_g = \frac{2\mu_g(\varepsilon - 1)}{a^3(\varepsilon + 2)} \tag{5}$$

This approach allows self-consistent feedback between the solvent reaction field and the polarizable solute dipole as in Onsager's model for the dielectric constant of polar liquids. Other proportional relationships ($\alpha = \varphi a^3$ with $\varphi < 1/2$) between cavity radius and polarizability have also been suggested, and predict slightly different solvatochromism. By combining equations 3 and 4 one obtains,

$$E_g = \beta \mu_g f(\varepsilon) \tag{6}$$

Where $\beta = 2/a^3$ and $f(\varepsilon) = (\varepsilon - 1)/(2\varepsilon + 1)$. Thus, the ground state energy, U_g, is stabilized by

$$U_g = -\mu_g E_e = -\left|\mu_g\right| \beta f(\varepsilon) \tag{7}$$

When the molecule is electronically excited, its dipole moment and charge distribution will instantly change. The solvent electronic polarization will also instantly adjust, but the solvent configuration (orientation, positions and intramolecular geometries) will not have time to change during the sudden absorption of light. This latter contribution to the solvent polarization which depends on nuclear positions is usually called orientational polarization. Thus, the initial reaction field after electronic excitation has an equilibrium electronic polarization for the excited state but an orientational polarization equilibrated to the ground state dipole. Before the nuclei can respond, the excited state (e) is affected by two fields:

$$E_e^0 = E_{g,nucl} + E_{e,elec} \tag{8}$$

Where $E_{g,nucl} = \beta \mu_g f(\varepsilon)$ is the reaction field from the orientational polarization alone, and $E_{e,elec} = \beta \mu_g f(n^2)$ is the field from the electrons. Thus, the initial (Franck-Condon) stabilization of the excited state, U_e is given by

$$U_e = -\mu_e (E_{g,nucl} + E_{e,elec}) = -\beta \mu_e \mu_g [f(\varepsilon) - f(n^2)] - \beta \left|\mu_e\right|^2 f(n^2) \tag{9}$$

The solvent shift in absorption wave number is thus

$$\begin{aligned} \Delta \tilde{\nu}_{abs} &= \frac{(U_e - U_g)}{hc} \\ &= \Delta \tilde{\nu}_{abs}^0 + \beta' \mu_g (\mu_g - \mu_e)\left(f(\varepsilon) - f(n^2)\right) + \beta' \mu_g \left(\left|\mu_g\right|^2 - \left|\mu_e\right|^2\right) f(n^2) \end{aligned} \tag{10}$$

Where $\beta' = \beta / hc$, and $\tilde{\nu}_{abs}^0$ is nominally a gas phase (solvent-free) absorption frequency. The term proportional to $(f(\varepsilon) - f(n^2))$ arises from the slow orientational solvent polarization while

the term proportional to $f(n^2)$ arises from the instantaneous electronic polarizability. A similar analysis beginning with the solvent equilibrated to the excited state yields a solvent shift in the emission wave number, $\tilde{\nu}_{em}$ given by

$$\Delta\tilde{\nu}_{em} = \Delta\tilde{\nu}^0_{em} + \beta'\mu_e(\mu_g - \mu_e)\left(f(\varepsilon) - f(n^2)\right) + \beta'\mu_g\left(|\mu_g|^2 - |\mu_e|^2\right) f(n^2) \qquad (11)$$

Note that the orientational polarization dependence of the emission spectrum differs from the absorption spectrum because the initial condition determines the solvent configuration after the transition. In contrast, the electronic polarization dependence is the same because it instantly adapts during the transition. If $\mu_g \| \mu_e$ and $|\mu_g| > |\mu_e|$, both absorption and fluorescence shift to the blue with increasing solvent polarity, but the absorption shifts are greater. Thus, the Stokes shift, $\Delta\tilde{\nu}_{ss}$, due to solvent polarity is given by the Lippert-Mataga equation as follows:

$$\Delta\tilde{\nu}_{ss} = \Delta\tilde{\nu}_{abs} - \Delta\tilde{\nu}_{em} = \frac{2}{4\pi\varepsilon_0 hca^{-3}}\left(\mu_e - \mu_g\right)\Delta f;$$

$$\Delta f = f(\varepsilon) - 0.5\, f(n^2) = \frac{\varepsilon - 1}{2\varepsilon + 1}\frac{1}{2}\frac{n^2 - 1}{2n^2 + 1} \qquad (12)$$

where Δf is the orientational polarizability. This expression of the Stokes shift depends only on the absolute magnitude of the charge transfer dipole difference $\Delta\mu = \mu_e - \mu_g$, and not on the angle between the dipoles. The validity of Eq. (12) can be checked by using various solvents and by plotting $\Delta\tilde{\nu}_{ss}$ as a function of Δf (the so called Lippert's plot). A linear plot is not always observed because only the dipole interaction is taken in to account and the solvent polarizability is neglected. By choosing solvents without hydrogen bonding donor or acceptor capability, a linear behavior is often observed, which allows determining the increase in dipole moment up on excitation, provided that a correct estimation of the cavity radius is possible. The uncertainties arise from the estimation of the Onsager cavity and from the assumption of a spherical shape of this cavity. For elongated molecules, an ellipsoid form is more appropriate. Inspite of these uncertainties, the Lippert-Mataga relation is widely used by taking the molecular radius as the cavity radius.

Non polar solvatochromism is usually described by a "general red-shift" attributed to dispersion interaction with the solvent is given by equations 13 and 14 for the absorption and emission wave numbers, respectively.

$$\Delta\tilde{\nu}_{abs} = \Delta\tilde{\nu}^{0}_{abs} - \gamma f(n^2) \quad (13)$$

$$\Delta\tilde{\nu}_{em} = \Delta\tilde{\nu}^{0}_{em} - \gamma f(n^2) \quad (14)$$

Where γ, the solvent polarizability, is the same for both absorption and emission because the electrons adjust instantaneously during the transition [42].

4. Experimental Details

4.1 Objectives

The general objective of this study is to investigate the origin of dual fluorescence of the newly synthesized DMABA-Amtr and solvent effects on the dual emission of the molecule. Specifically, the aim is

a) to identify which equilibrium state (ground or excited) is responsible for the dual emission observed in DMABA-Amtr,
b) to examine the effect of nonpolar and polar solvents on the absorption, excitation and emission spectra of the molecule and finally
c) to predict the change in dipole moment of the molecule during absorption of light quanta.

4.2 Materials and Methods

All the solvents used in this study are spectroscopic grade. The compound (E)-N-(4-(dimethylamino) benzylidene)-2H-1,2,4-triazol-3-amine (DMABA-Amtr) shown in Schem I, is kindly supplied by Mr. Belina.

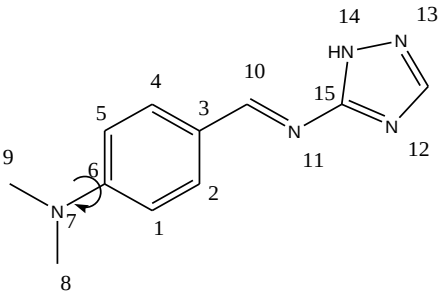

Schem I Chemical structure of the investigated compound DMABA-Amtr.

Absorption measurements were made using a SPECTRONIC GENESYS 2PC UV-Vis spectrophotometer. Emission and excitation spectra were recorded with Fluoromax-4 spectrophotometer. Solvent blanks were subtracted from the absorption and emission spectra prior to analysis. Emission spectrum was recorded by fixing the excitation wavelength and varying the emission wavelength, while excitation spectrum was recorded by fixing the emission wavelength and scanning the excitation wavelength. Post data processing was done by using

Origin.6 software. In the data analysis, the Raman and Rayleigh peaks were subtracted from the excitation and emission spectra.

4.3 Computational Details

The minimum ground state structure of DMABA-Amtr is obtained by optimizing more the geometry at DFT level with B3LYP functional and 6-31G basis set using Gaussian 03 package [5, 17]. Molecular mechanics was used for potential energy surface (PES) calculation in polar solvents. MM+ force field calculation was performed using Hyperchem 7.5 software. This was done by rotating the dimethyl amino group (-NMe_2) between torional angles of 0^0 and 180^0 in periodic cubic box of length 25.73873 Å that contains 564 water molecules (polar environment).

5. Result and Discussion

5.1 Emission spectra

A series of emission spectra of DMABA-Amtr were obtained at different excitation wavelengths in solvents of different polarities. The effect of solvent polarity and variation of excitation wavelength on the emission behavior are also investigated. The fluorescence spectra of DMABA-Amtr in solvents of different polarities are presented in Fig.8a.

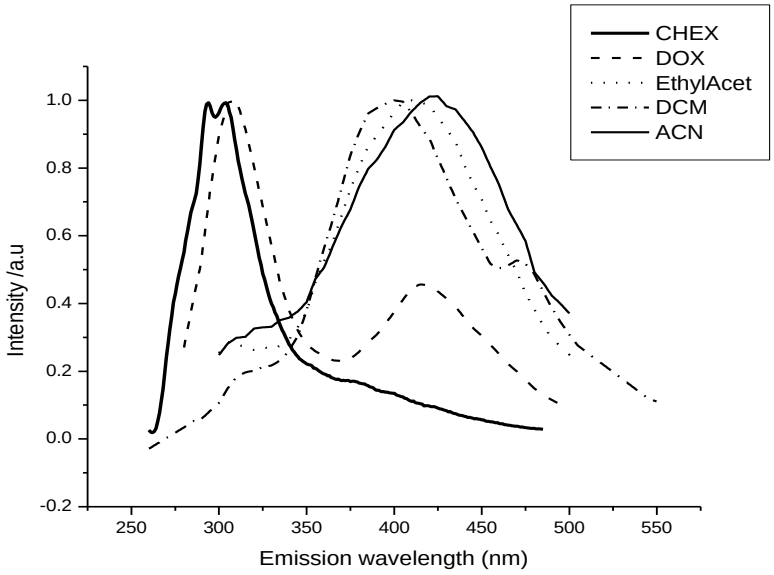

Fig.8a Peak normalized emission spectra of DMABA-Amtr in solvents of different polarities at excitation wavelength λ_{Exc} = 260 nm.

As can be seen from the figures, the emission spectra of the molecule are very much influenced by solvent polarity as well as the wavelength of excitation. The corresponding peak positions are listed in Table 1.

Table 1 Values of fluorescence emission maxima of DMABA-Amtr in solvents of different polarities.

Solvent	LE em (nm)	LE em (cm^{-1})	CT em (nm)	CT em (cm^{-1})	Δf
Cyclohexan	305	32786	-	-	0.10037
Dichloromethane	315	31746	470	21276	0.31878
Acetonitrile	315	31746	446	22421	0.39199
Dioxane	310	32258	415	24096	0.28324
Ethylacetate	310	32258	423	23640	0.29230
Hexanol	310	32258	430	23255	-

5.1.1 Emission spectra in Cyclohexane

Emission spectra of DMABA-Amtr were recorded as a function the excitation wavelength in a solution of cyclohexane are presented in Fig.8b.

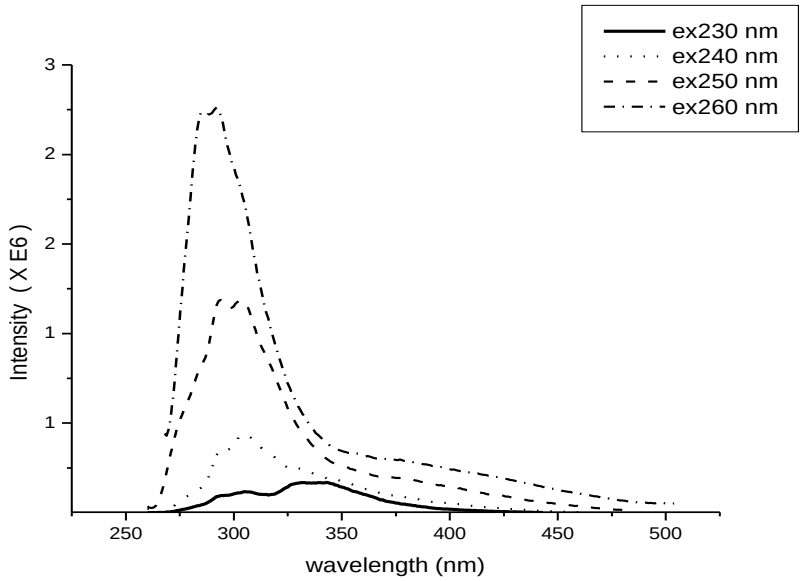

Fig.8b Emission spectra of DMABA-Amtr in cyclohexane at different excitation wavelengths.

Only the band of the locally excited state emission centered at $\lambda_{em} = 300$ nm is observed, and the shape and position of the spectrum is found to be independent of the excitation quanta up on changing the excitation wavelength from 230 to 260 nm.

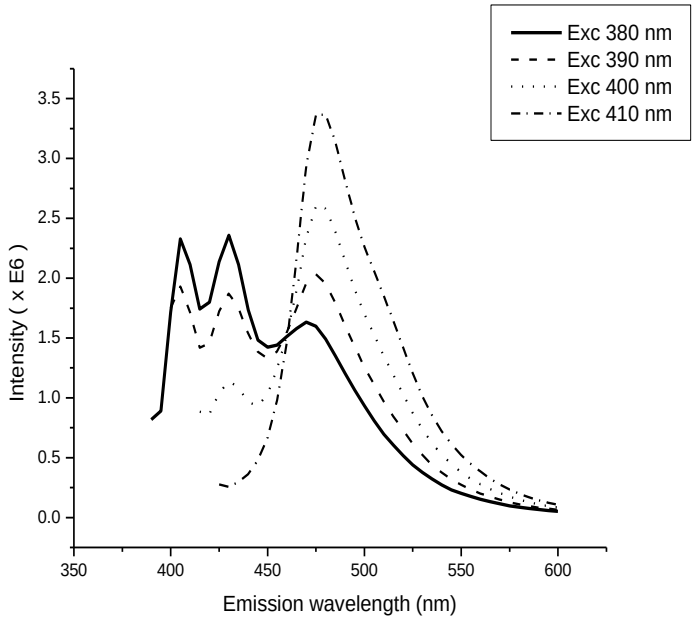

Fig. 9 Emission spectra of DMABA-Amtr in dichloromethane.

The situation is, however, different for DMABA-Amtr in polar solutions. The fluorescence spectrum of the solution of dichloromethane (Fig. 9), for instance, consists of two bands centered at $\lambda_{em} = 405$ nm nm and $\lambda_{em} = 470$ nm . From the figure it is observable that the intensities of the two emissions seem to depend significantly on the excitation wavelength. Increasing the excitation wavelength leads to change in the intensity ratio of the two bands, indicating that the bands represent the emitting levels originating from two different electronic states. The plot of intensity ratio (I_{LE} / I_{CT}) versus excitation wavelength and a table of values of intensity ratio for the LE and CT emissions are presented in Table 2 and Fig.10, respectively.

Table 2 Values of fluorescence emission intensities of DMABA-Amtr for the LE emission and CT emission in dichloromethane

λ_{Exc} / nm	I_{LE} / a.u.	I_{CT} / a.u.	I_{LE}/I_{CT}
380	232	164	1.419
390	190	203	0.939
400	819	258	0.317
410	326	335	0.097

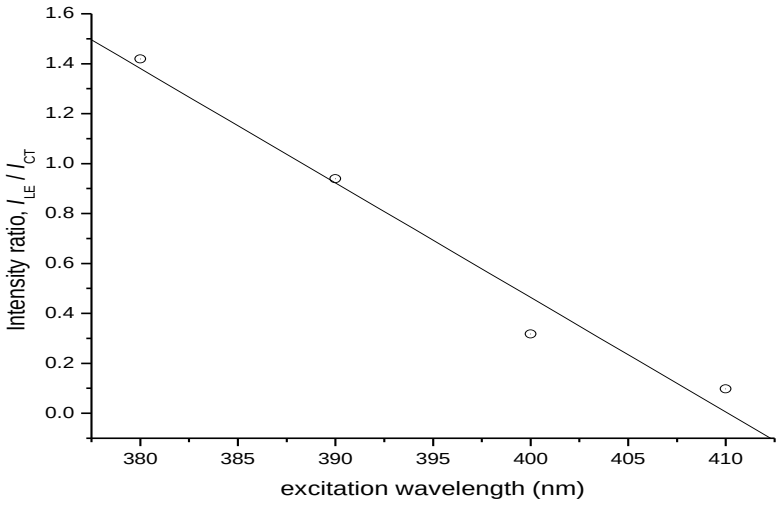

Fig.10 Plot of I_{LE} / I_{CT} versus excitation wavelength of DMABA-Amtr in dichloromethane.

The plot clearly shows the ratio of the intensity maxima of the components I_{LE} / I_{CT} decreases in favor of the CT band. This excitation wavelength dependence of the intensity ratio does not represent an emission from the vibronic levels, in which case the I_{LE} / I_{CT} ratio should not vary significantly, rather suggests the existence of more than one structure in the ground state which are responsible for the observed dual emission. The most interesting property of spontaneous emission by DMABA-Amtr is the unusually strong dependence of emission bands on the exciting light wavelength in the range 380 – 410 nm in dichloromethane. The character of the changes relates to both emission bands and appears as follows. First, the ratio of the intensity

maxima of the components, I_{LE} / I_{CT}, decreases in favor of the CT band as the excitation wavelength increase from 380 - 410 nm.

Detailed analysis of excitation wavelength dependence of the emission band in dichloromethane solution is done by collecting emission spectra in the blue-edge range (310 - 340 nm), red-edge (410 - 450 nm) and in the middle wavelength range (380 - 410 nm), and the corresponding spectra are presented in Fig.11, 12 and 13, respectively.

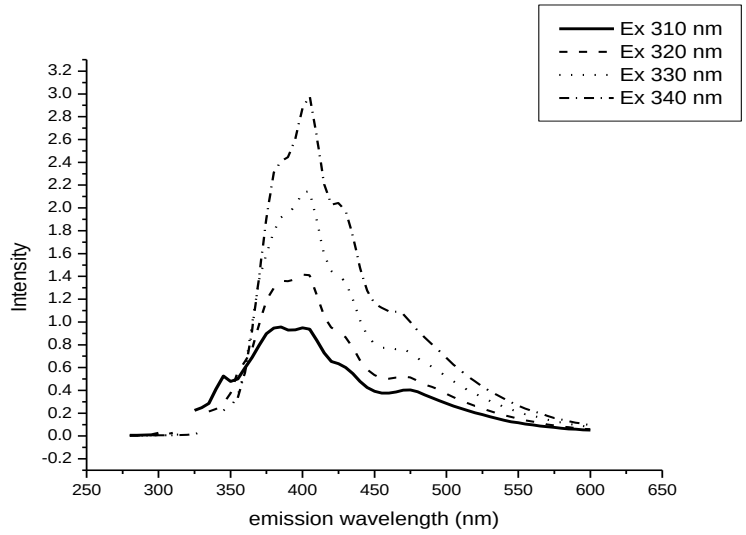

Fig.11 Emission spectra of DMABA-Amtr in dichloromethane solution in wavelength range 310-340 nm (blue-edge).

In Fig.11, excitation of the molecule in the blue-edge of excitation gives predominantly an LE emission (single band) centered at λ_{em}= 370 nm, indicating excitation of a single species in this wavelength range.

A similar result, i.e. a single emission band, is found by excitation of the molecule in the red-edge range (410 - 450 nm) (Fig.12).

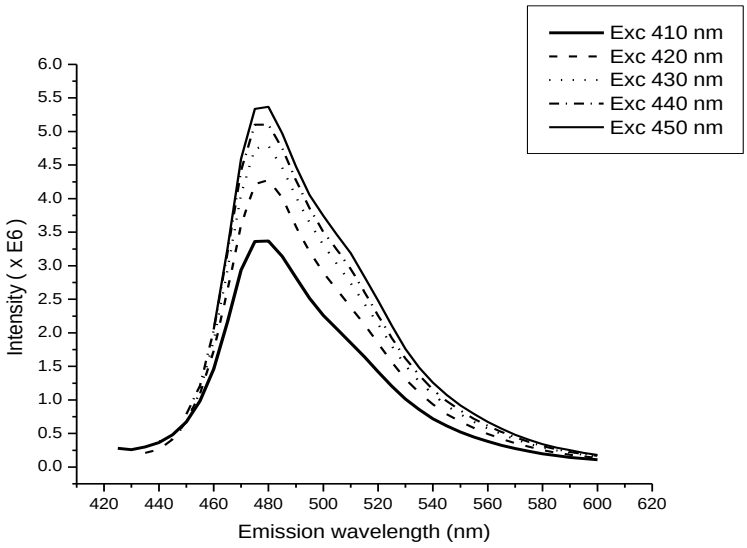

Fig.12 Emission spectra of DMABA-Amtr in dichloromethane solution in wavelength range 410-450 nm (red-edge).

In Fig.12, increment of the excitation wavelength to the longer wavelength side causes an increment in the CT band at the expense of the LE band. Excitation of the molecule at this wavelength range essentially gives the CT emission band with a small shoulder corresponding to the LE band. In this case, the emission wave length is centered at λ_{em} = 470 nm, still indicating the excitation of a single species at the excitation wavelength range 410-450 nm (red-edge).

The situation becomes completely different when the molecule is excited in the wave length range 410 - 450 nm (Fig.13). Excitation of the molecule in the wavelength range 380 - 410 nm gives dual emission centered at λ_{em} = 370 nm and λ_{em} = 470 nm. This observation is, however, in contrast to the Kasha Rule stating that the same emission spectrum is generally observed irrespective of the excitation wavelength; i.e. a single excitation band gives rise to a single emission spectrum. Deviation from the Kasha rule, like the case encountered, can be attributed to various reasons.

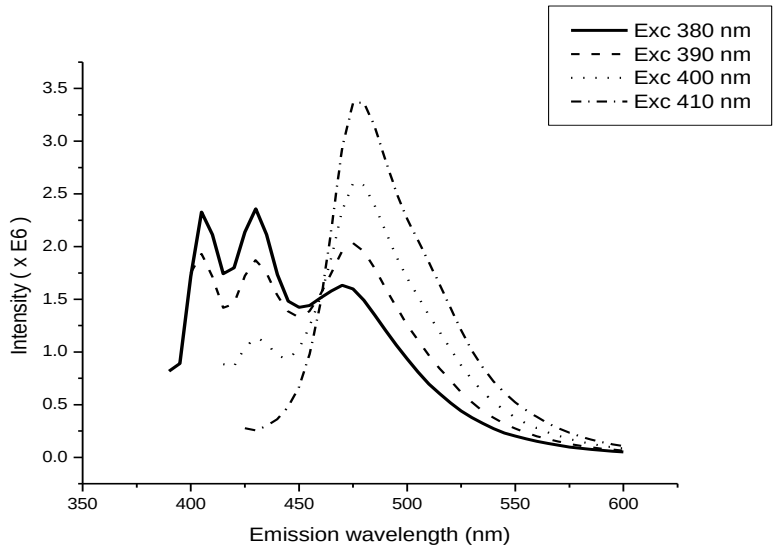

Fig.13 Emission spectra of DMABA-Amtr in dichloromethane solution in wavelength range 380-410 nm.

Dual emission, generally, can have its origin from (a) concentration dependent aggregation of molecules in the ground or excited state, (b) two modes of electronic transitions, (c) the presence of two different compounds in the ground or excited state and (d) the presence of two different structures of the same molecule.

In our case, measurement of the absorption and fluorescence spectra are done at very low concentrations in such a way that the absorbance and fluorescence are adjusted to be less than 1 and 0.2, respectively, so that formation of molecular aggregate is prohibited. Hence option (a) cannot be the origin of the dual emission observed in DMABA-Amtr. Option (b) and (c) cannot also be the origins of the dual emission observed in our case because had the dual emission been from two modes of transitions, (b) or from the presence of two different compounds in the ground or excited state, (c), then there would not have been excitation wavelength dependence. However, in our case a significant excitation wavelength dependence of the two emission spectra is observed. Hence, option (d), the presence of two different structures of the same molecule, is the most likely reason for the observed dual emission in DMABA-Amtr.

Estimation of the number of possible stable structures was carried out by area normalization of the emission spectra of DMABA-Amtr in dichloromethane and the result is presented in Fig.14.

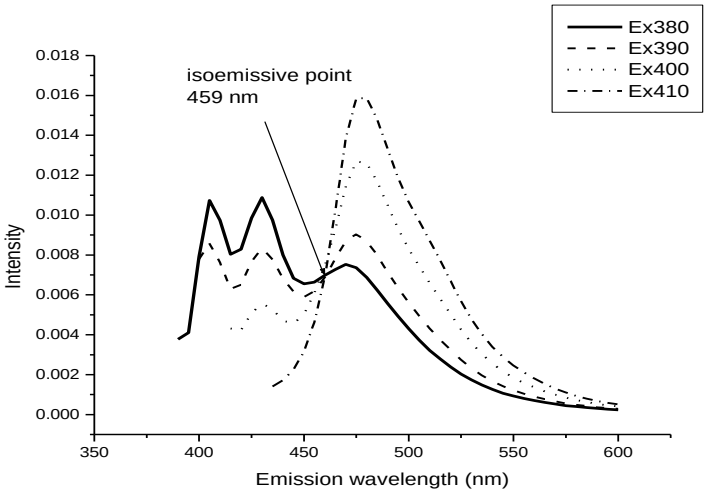

Fig.14 Area normalized emission spectra of DMABA-Amtr in dichloromethane.

From the figure, a single isoemissive point is observed at about λ_{Em} = 459 nm, indicating only two emissive species in the excited state originating from a single compound in the ground state giving rise to two different structures. To further verify the results, 3D emission spectral studies were performed. The 3D spectra recorded for DMABA-Amtr in cyclohexane and dioxane solutions are shown in Fig.15 and 16, respectively.

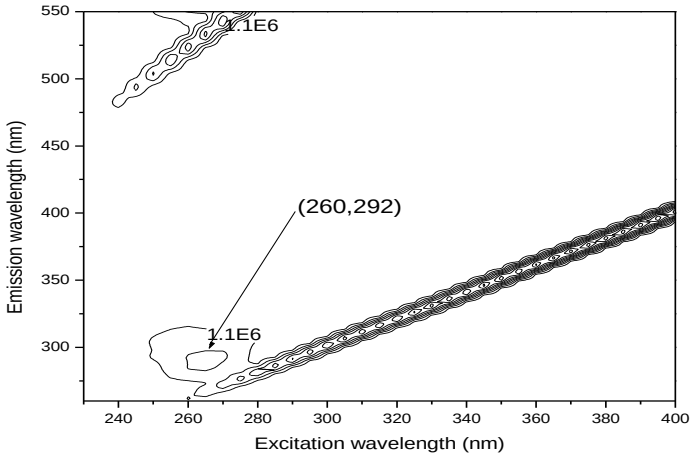

Fig.15 3D spectra of DMABA-Amtr in cyclohexane.

In a nonpolar solvent, cyclohexane, the 3D spectra of DMABA-Amtr gives only one contour. The corresponding excitation spectrum shows only one band at 260 nm and the emission spectrum shows an emission at 292 nm indicating the presence of only one stable species in the ground state. On the other hand, a different situation is observed in the 3D spectra of DMABA-Amtr in dioxane solution (Fig.16).

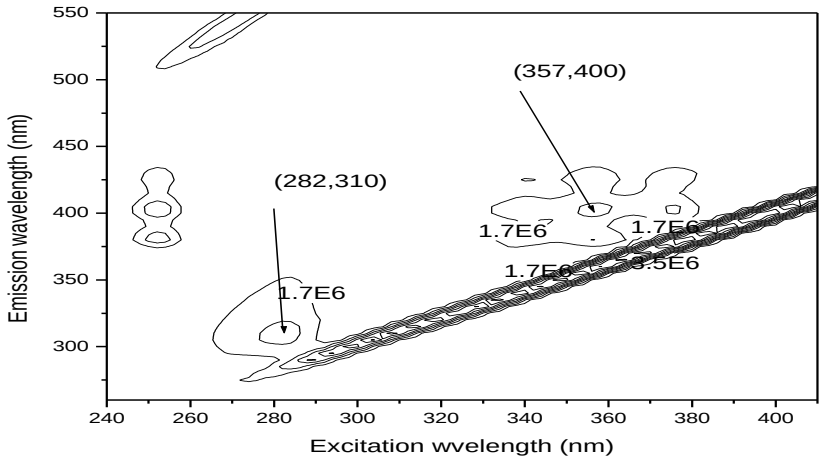

Fig.16 3D spectra of DMABA-Amtr in dioxane solution.

As shown in the figure, the 3D spectra of DMABA-Amtr show two contours in a polar solvent, dioxane. The first excitation band at λ_{Exc} = 282 nm corresponds to the emission at λ_{Em} = 310 nm and the second excitation band at λ_{Exc} = 357 nm corresponds to the second emission at λ_{Em} = 400 nm. The results show that the excitation band observed at 282 nm corresponds to the LE emission at 315 nm and the excitation band observed at 357 nm corresponds to the CT emission at 400 nm. The two excitation spectra resolved for the corresponding emission spectra of DMABA-Amtr in a solution of dichloromethane is shown in Fig.17.

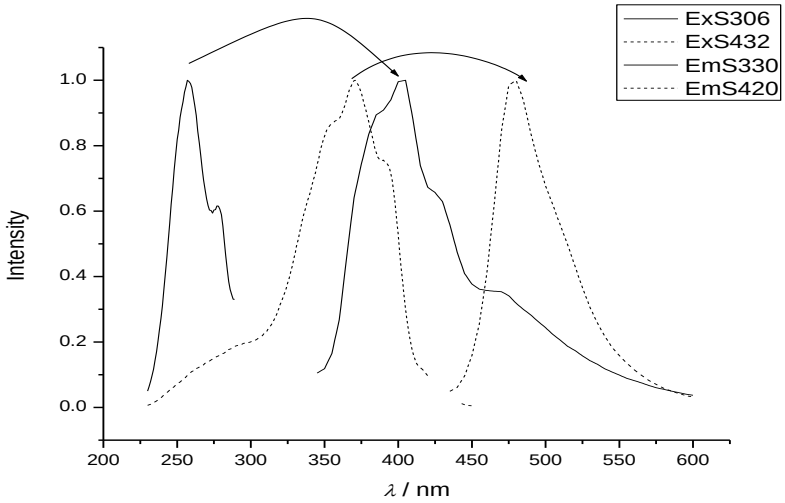

Fig.17 Peak normalized excitation and corresponding emission spectra of DMABA-Amtr in dichloromethane.

From the figure, it seems that the emission spectra centered at λ_{Em} = 370 nm originate from the excitation spectra at around λ_{Exc} = 257 nm and the emission spectra centered at λ_{Em} = 470 nm originate from the excitation centered at λ_{Exc} = 355 nm.

The excitation and 3D spectra confirms the presence of two species of the same molecule in the ground state. The overlapping of the electronic absorption spectra of the two species leads to the dual fluorescence of the compound at all wavelengths of excitation in the region 380 nm to 410 nm. At the blue edge of excitation, LE state fluorescence dominates but at the red-edge of excitation, the CT state emission dominates; showing that one can independently excite the two structures by selecting the appropriate wavelength region.

Similar results are found for the compound in another polar solvent, acetonitrile. In this case, however, the CT emission is predominant (as the solvent is highly polar and hence stabilizing the CT state more), and the LE emission is appearing only as a shoulder (Fig18).

.

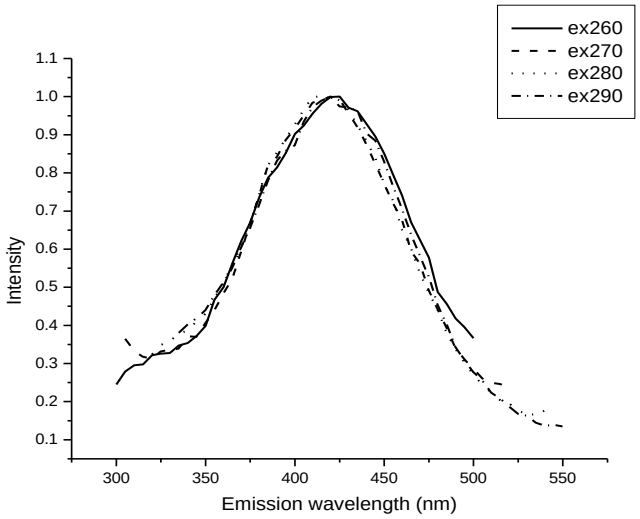

Fig.18 Peak normalized emission spectra of DMABA-Amtr in acetonitrile in excitation wavelength range 260 - 290 nm.

As shown in the figure, excitation of the molecule in the wavelength range 260 - 290 nm gives dual emission in which the CT emission is predominant centered at λ_{Em} = 445 nm and the LE emission appearing as a shoulder centering at λ_{Em} = 315 nm, indicating better stabilization of the CT state in highly polar solvents like acetonitrile.

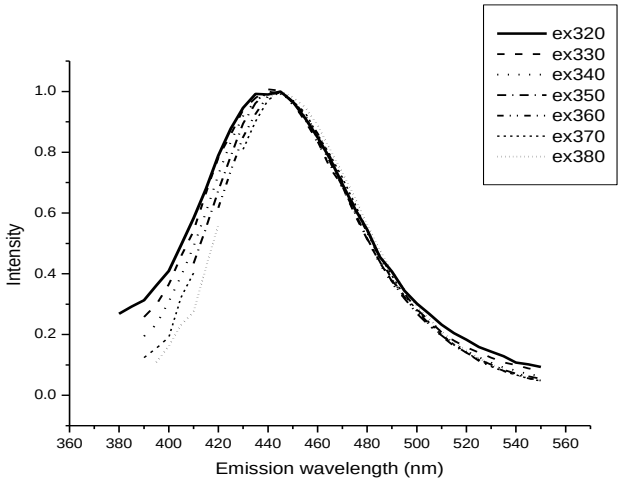

Fig.19 Peak normalized emission spectra of DMABA-Amtr in acetonitrile in excitation wavelength range 320 - 380nm.

In Fig.19, Further increment of the excitation wavelength essentially gives the CT band indicating the predominant structure of the molecule in polar solvents is the one with a charge transfer character. The area normalized emission spectra of DMABA-Amtr in acetonitrile solution is presented in Fig.20.

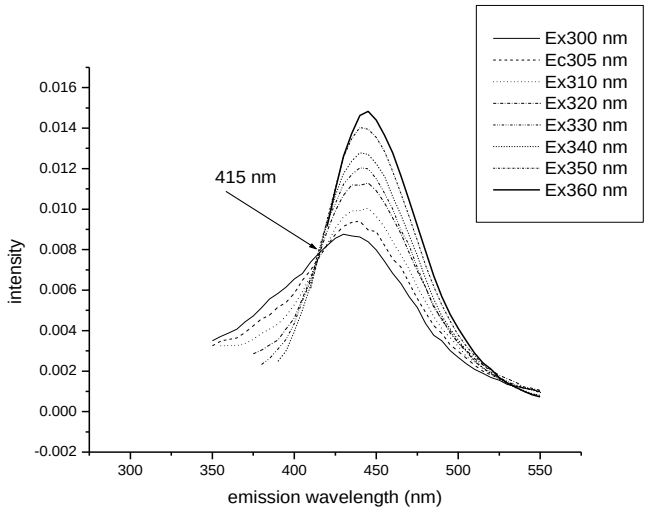

Fig.20 Area normalized emission spectra of DMABA-Amtr in acetonitrile.

As shown in the figure, the area normalized excitation spectra in the wavelength range 300 nm-360 nm gives a single isoemissive point centered at λ_{Em} = 415 nm, indicating two emitting states originating from two equilibrium structures of a molecule in the ground state.

5.2 Excitation Spectra

The excitation spectra of DMABA-Amtr for solutions of different polarities were monitored at different emission wavelengths. The excitation spectra of DMABA-Amtr are found to be almost independent of the emission wave length in a nonpolar solvent, cyclohexane, whereas the excitation spectra are found to be highly dependent on the emission wavelength in polar solvents. The excitation spectra of DMABA-Amtr in solutions of cyclohexane and dichloromethane are presented in Figs. 21 and 22.

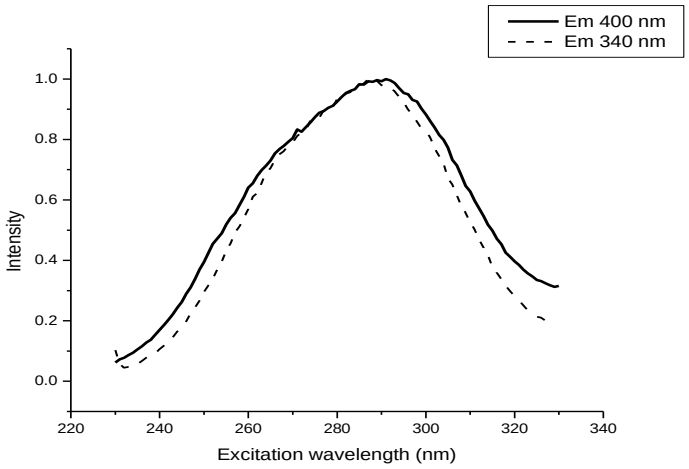

Fig.21 Peak normalized excitation bands of DMABA-Amtr in cyclohexane at different emission wavelengths.

In Fig.21, the excitation spectra of DMABA-Amtr collected at different emission wavelengths (λ_{Em} = 300 nm, 340 nm and 400 nm), did not show significant deviations both in position and shape of the excitation spectra. The excitation bands found are centered at λ_{Exc} = 280 nm. The results indicate either the presence of a single stable species or two exchangeable close lying structures of the same molecule.

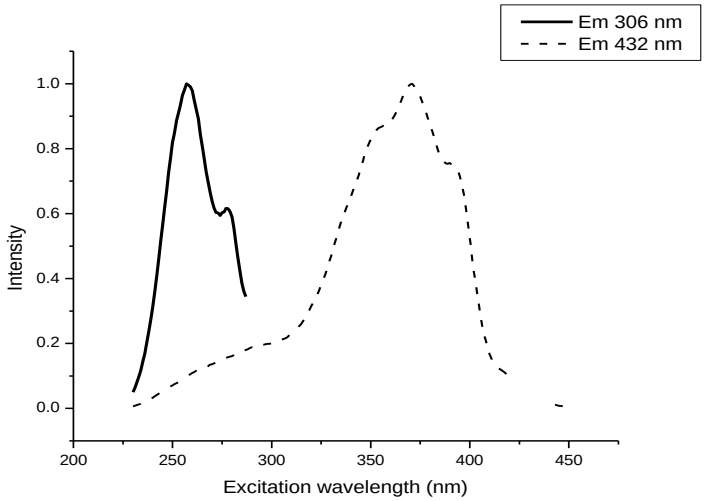

Fig.22 Peak normalized excitation bands of DMABA-Amtr in dichloromethane at different emission wavelengths.

The excitation spectra of the molecule in polar solvents are, however, found to be highly dependent on the emission spectra. In dichloromethane solution, for example, two distinct excitation spectra are found by excitation of the molecule at different emission wavelengths (Fig.22). As shown in the figure, the excitation spectrum fixed at emission wave length of λ_{Em} = 306 nm is centered at λ_{Exc} = 257 nm and the second excitation spectrum collected at emission wavelength of λ_{Em} = 432 nm is centered at λ_{Exc} = 355 nm. The result indicates the presence of two stable structures in the ground state. The excitation spectra at the two different emission bands show discrepancies from the absorption spectra (Fig.23).

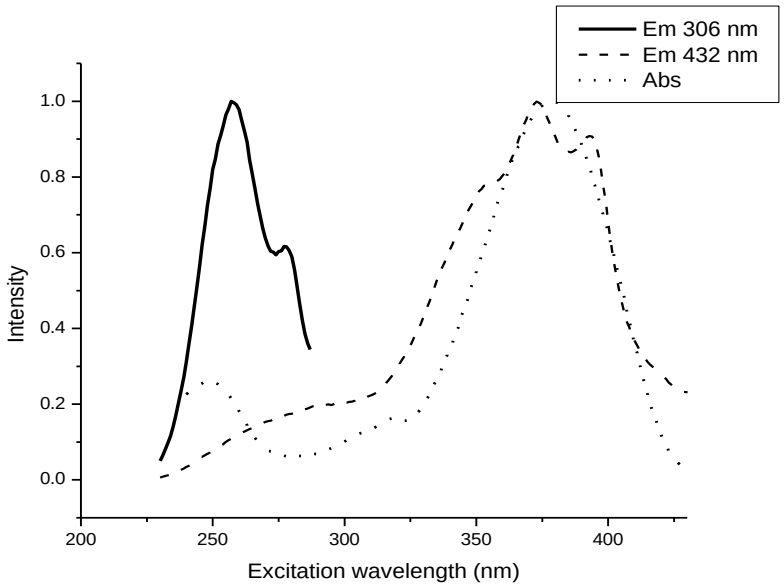

Fig.23 Peak normalized excitation and absorption spectra of DMABA-Amtr in dichloromethane solution.

In Fig.23, the absorption spectrum seems to be a combination of the two excitation spectra, each coming from different species in the ground state. This result further supports the presence of two stable ground state structures of the molecule in polar solvents.

Similar situation is also observed in another polar solvent, acetonitrile; i.e. the excitation spectra are found to be highly dependent on the emission wavelength (Fig.24).

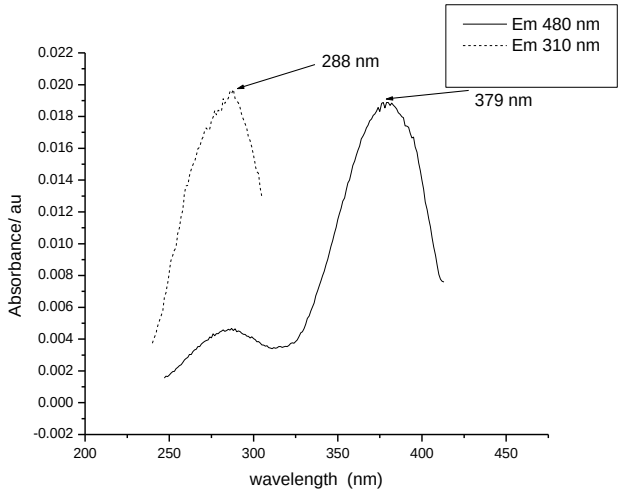

Fig.24 Excitation spectra of DMABA-Amtr taken at different emission wavelength in acetonitrile solution.

In Fig.24, two distinct excitation spectra centered at 288 nm and 379 nm are observed for fixed emissions at 310 nm and 480 nm, respectively. The result still supports the presence of two stable ground state conformers of the molecule. Similar to the solution of dichloromethane, the two excitation bands in acetonitrile show discrepancy from the corresponding absorption band (Fig.25).

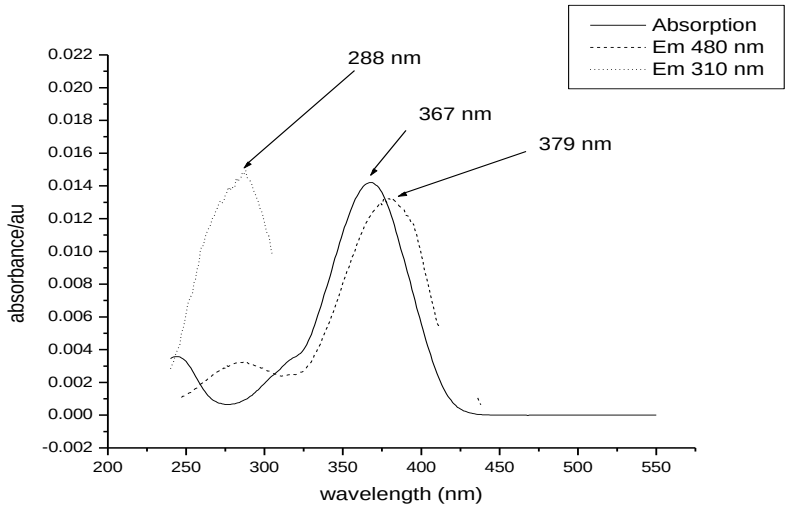

Fig.25 Excitation and absorption spectra of DMABA-Amtr in acetonitrile solution.

The absorption spectrum (Fig.25) still seems to be a combination of the two excitation spectra, each coming from different species in the ground state. This result can be a good evidence for presence of two stable ground state structures of the molecule in the polar acetonitrile solution.

Resolution of the absorption spectra of DMABA-Amtr in Acetonitrile shows two distinct absorbances whose values correspond to the two excitation bands (Fig.26)

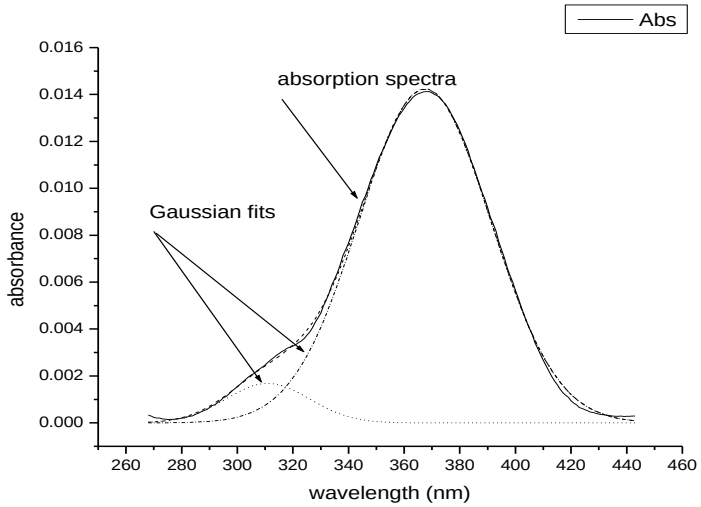

Fig. 26 Gaussian Fit of absorption spectra of DMABA-Amtr in acetonitrile solution.

From the figure, it can be shown that the smaller band corresponds to the excitation band at higher energy and the more intense band corresponds to the lower energy excitation band.

5.3 Absorption spectra

A series of absorption spectra of DMABA-Amtr were recorded in cyclohexane, 1,4-dioxane,dichloromethane, and acetonitrile solutions in order to study the role of solvent polarity in modifying the electronic states of the compound (Fig.27). More comprehensive data is summarized in Table 3.

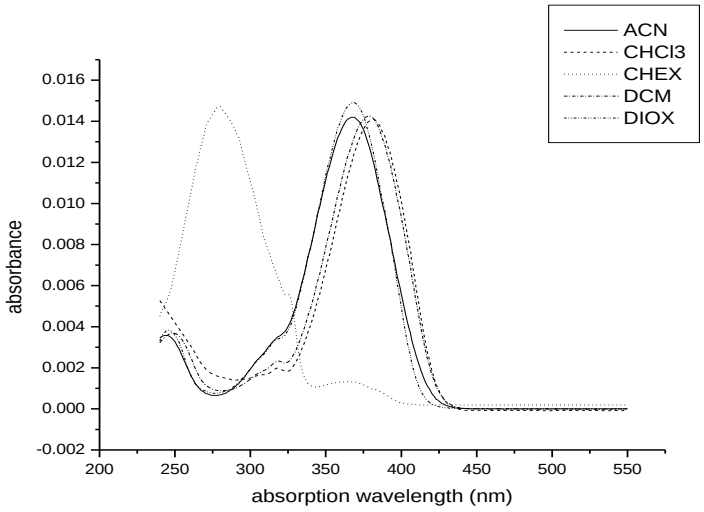

Fig.27 Absorption spectra of DMABA-Amtr in solvents of different polarities.

Table 3. Values of absorption maxima of DMABA-Amtr in solvents of different polarities.

Solvent	ε	n	Δf	E_T	λ_{max} **(nm)**
Cyclohexane	2.02	1.4262	0.10037	0.006	279
Chloroform	4.89	1.4459	0.25561	0.259	381
Dichloroethane	10.36	1.4448	0.32587	0.327	375
Dichloromethane	8.93	1.4242	0.31878	0.309	378
Diethylether	4.2	1.3524	0.25144	0.117	365
Dioxane	6	1.4224	0.29230	0.164	368
Acetonitrile	35.94	1.3441	0.39199	0.46	367
Ethylacetate	6.02	1.3724	0.29230	-	367
Methanol	32.66	1.3284	0.39297	0.762	374
Ethanol	24.55	1.3614	0.3794	0.654	348
2-propanol	82.2	1.3772	0.3974	0.546	371
Butanol	17.51	1.3993	0.36092	0.586	374
Pentanol	13.9	1.41	0.34863	0.568	377

The absorption spectra of DMABA-Amtr in solvents of various polarities (cyclohexane, 1,4-dioxane, chloroform, dichloromethane and acetonitrile) has been examined and the results are presented in Fig.20. From the figure, it can be seen the absorption maxima shifts from 279 nm in cyclohexane solution to 367 nm in acetonitrile solution and the absorption λmax is found to generally increase with increasing solvent polarity (bathochromic shift). The bathochromic shift generally shows an increase in the permanent dipole moment of the excited state than the ground state.

The solvatochromic shift of the absorption maxima ν_{abs} (cm^{-1}) generally follows functional dependence on the solvent dielectric constant ε, and refractive index n, given by the equation:

$$\tilde{\nu}_{abs}^{sol} = \tilde{\nu}_{abs}^{0} - \frac{2\mu_g(\mu_e - \mu_g)}{4\pi\varepsilon_0 hca^3}\left[\frac{\varepsilon - 1}{2\varepsilon + 1} - \frac{1}{2}\frac{n^2 - 1}{2n^2 + 1}\right] \qquad (19)$$

where h is Plank's constant, c is the speed of light, ν_{abs}^{sol} and ν_{abs}^{o} are the solvent equilibrated absorption maxima and the value extrapolated to gas phase conditions, respectively; the superscript "0" indicates the absence of a solvent (free molecule), μ_g and μ_e are the ground and excited-state dipole moments, a is the radius of the Onsager cavity, ε is the static dielectric constant, and n is the optical refractivity index of the solvent. The approximation used (rigid point dipole in the center of a spherical Onsager cavity) neglects the polarizability of the solute.

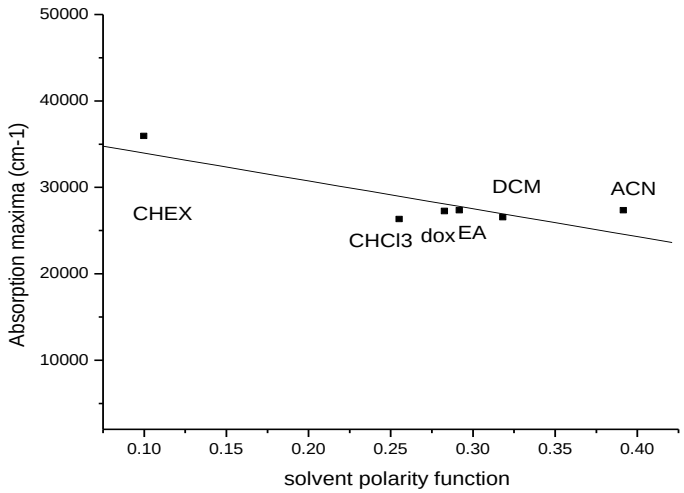

Fig.28 Plot of absorption maxima (in wave number) versus solvent polarity function (CHEX: cyclohexane; $CHCl_3$: chloroform; dox: 1,4-dioxane; EA: ethylacetate; DCM: dichloromethane and CAN: acetonitrile).

The solvatochromic shift of the absorption maxima in wave number plotted against solvent polarity functional, $(\varepsilon-1)/(2\varepsilon+1)-(0.5)(n^2-1)/(2n^2+1)$, is presented in Fig.28.

The Solvatochromic shift of the absorption maxima plotted against solvent polarity functional shows a sort of scattering and this may be due to polarization effect, which is refractive index functional, more significant in $CHCl_3$ and dichloromethane. Also the plots of absorption maxima as a function of dielectric constant functional, $f(\varepsilon)=(\varepsilon-1)/(2\varepsilon+1)$, and refractive index functional, $f(\varepsilon)=(n^2-1)/(2n^2+1)$ are considered separately. Improved linear dependence is obtained when the two functional are treated independently as shown in Figs. 29 and 30, respectively.

Fig.29 presents plot of the absorption maxima versus solvent dielectric function. The plot shows improved linear dependence of the absorption maxima with the dielectric function.

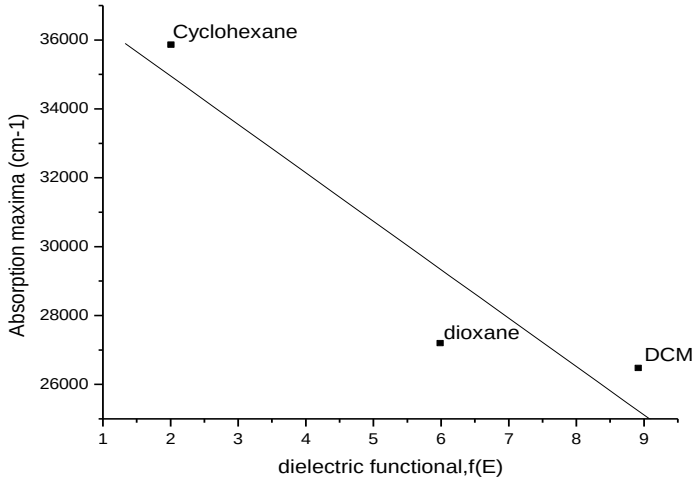

Fig.29 Plot of absorption maxima versus solvent dielectric function.

Similarly, an improved linear dependence of the absorption maxima is found with the refractive index function (Fig.30).

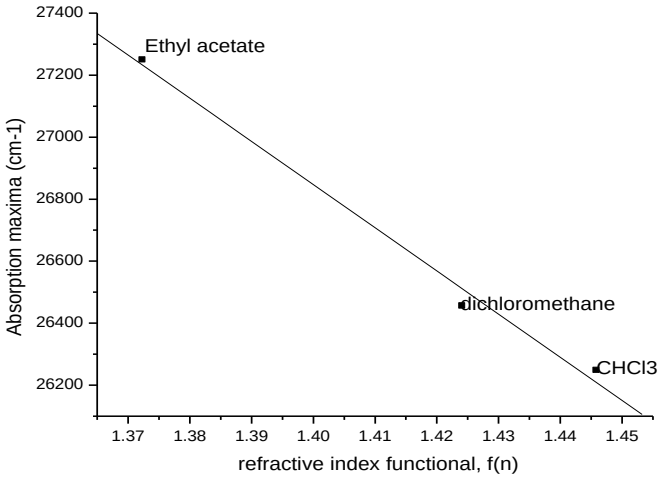

Fig.30 Plot of absorption maxima versus solvent refractive index function.

The difference in absorption maxima between the highly dipolar solvent acetonitrile and that in polar solvent cyclohexane is almost the same as between that of the highly polarized chloroform and cyclohexane, indicating that the effects of dielectric interaction are greater.

5.4 Solvatochromic Shifts and Excited State Dipole Moments

In general, emission bands result from excitation bands, and excitation bands are similar to absorption bands. However, in cases where there is a difference between absorption and excitation bands, it is appropriate to consider excitation spectrum rather than absorption spectrum. In our case, the absorption spectra of DMABA-Amtr may be considered as an overlap of two excitation spectra and thereby, the two excitation maxima are taken instead of the absorption maxima in equation 5. Thus, replacing $\tilde{\nu}_{abs}$ by $\tilde{\nu}_{Exc}$, the equation becomes:

$$\tilde{\nu}_{Exc-1}^{sol} = \tilde{\nu}_{Exc-1}^{0} - \frac{2\mu_g(\mu_{e1}-\mu_g)}{4\pi\varepsilon_0 hca^3}\left[\frac{\varepsilon-1}{2\varepsilon+1} - \frac{1}{2}\frac{n^2-1}{2n^2+1}\right] \qquad (20)$$

For the first excitation band and

$$\tilde{\nu}_{Exc-2}^{sol} = \tilde{\nu}_{Exc-2}^{0} - \frac{2\mu_g(\mu_{e2}-\mu_g)}{4\pi\varepsilon_0 hca^3}\left[\frac{\varepsilon-1}{2\varepsilon+1} - \frac{1}{2}\frac{n^2-1}{2n^2+1}\right] \qquad (21)$$

The plots of excitation wave number for the first and second excitation maxima versus solvent polarity functional, $f(\varepsilon)-(0.5)f(n)$, are given in Figs. 31 and 32 respectively. A comprehensive data value is included in Table 4.

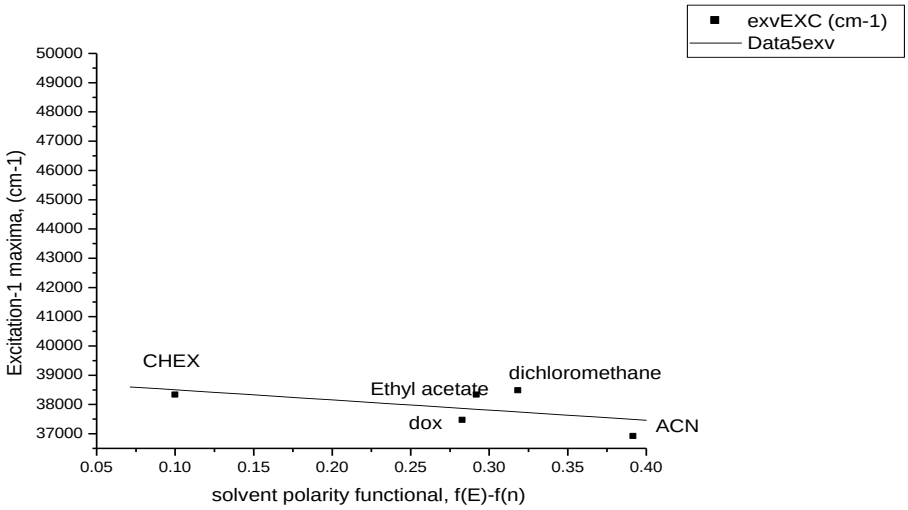

Fig.31 Plot of excitation wave number-1 versus solvent polarity function.

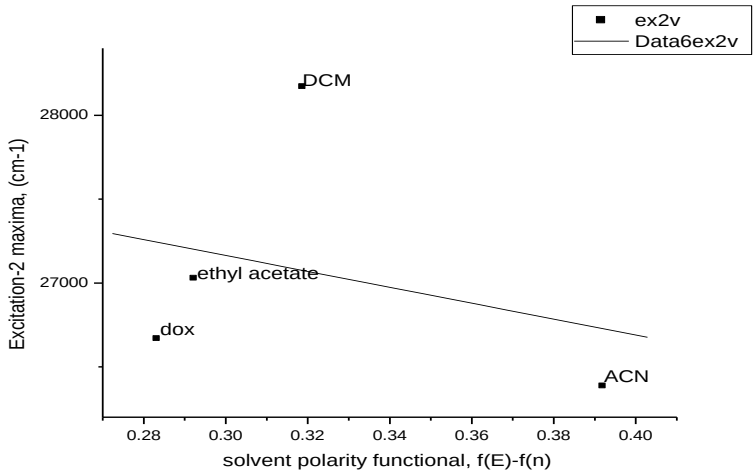

Fig.32 Plot of excitation wave number-2 versus solvent polarity function.

In the figure above, the plot of the first excitation wave number versus solvent polarity function shows a very gentle slope (-3468 cm^{-1}). The first excitation maxima shifts from 261 nm in cyclohexane to 270 nm in acetonitrile (change of 6 nm only!), indicating there is no appreciable

dipole moment change in the excited molecule for the conformer corresponding to the first excitation energy. The solvent polarity dependence of the second excitation energy is also examined and the result is presented in Fig.32.

Table 4 Values of the absorption, excitation and emission maxima of DMABA-Amtr in solvents of different polarities.

Solvent	**abs**	**Exc_1**	**Exc_2**	**Em_1**	**Em_2**	**Δf**	**$Exc_1 - Em_1$ (cm^{-1})**	**$Exc_2 - Em_2$ (cm^{-1})**
CHEX	279	261		305		0.10037	5527.3	-
DCM	378	260	355	315	470	0.31878	6715.5	6892.4
ACN	367	270	379	315	446	0.39199	5291.0	3963.7
Diox	368	267	375	310	415	0.28325	5195.1	2570.3
Ethylacet	367	260	370	310	423	0.29230	6203.5	3386.4
$CHCl_3$	381							
DEE	365							
DCE	375							

In Fig.32, there is still a gentle slope (but steeper than the first solvatochromic shift having a slope value of -4740 cm^{-1}). The solvatochromic shift, red-shift, shows an increase in dipole moment in the excited state.

Solvatochromic effects are also examined for the emission spectra. The solvent polarity dependent shift of the first and the second emission bands in solvents of different polarities are tested and the results are presented in Figs. 33 and 34.

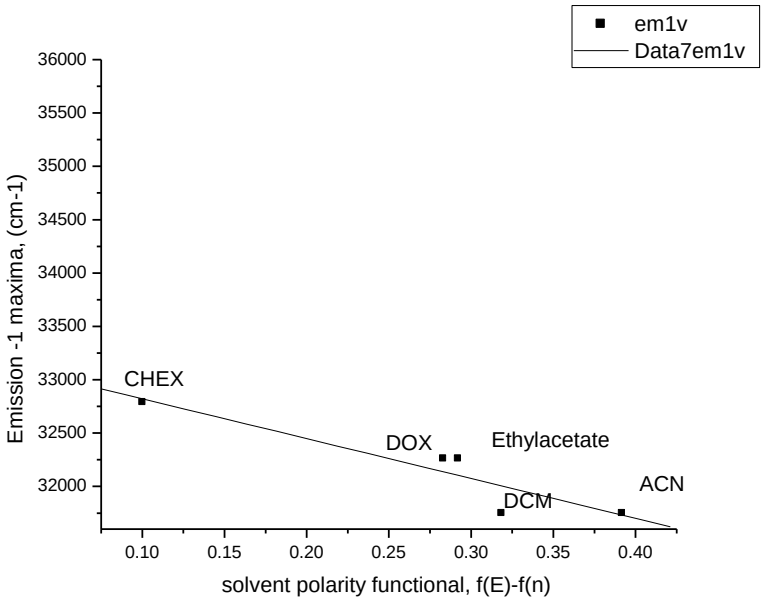

Fig.33 Plot of emission wave number-1 versus solvent polarity function

In Fig.33, plot of the first emission maxima against solvent polarity function gives a slope of -3736 cm^{-1}. This value is almost similar to the first excitation wavelength dependence on solvent polarity (-3468cm^{-1}). These results shows that the dipole moment of the conformer excited at lower wavelength did not appreciably change in the excited state, i.e. $\mu_{g1} \approx \mu_{e1}$, where μ_{g1} and μ_{e1} are the ground state and excited state dipole moments of the first transition (conformer 1), respectively.

The plot of the second emission maxima against solvent polarity parameter is presented in Fig. 34.

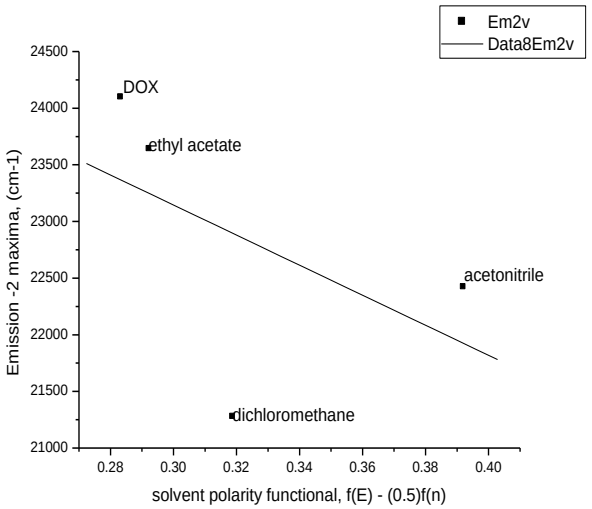

Fig.34 Plot of emission wave number-2 versus solvent polarity function.

From the plot above, the slope of the second emission maxima against solvent polarity is found to be -14569 cm^{-1}. The slope is significantly different from that of the first emission indicating the second emitting state is of higher dipole moment and involving greater charge transfer.

Application of Lippert-Mataga equation shows the extent of solvent polarity dependent stokes shift observed for the first (LE) emission and the second (CT) emission. Plots of the Stokes shift for the LE emission and CT emission versus solvent polarity function are presented in Figs.35 and 36 respectively.

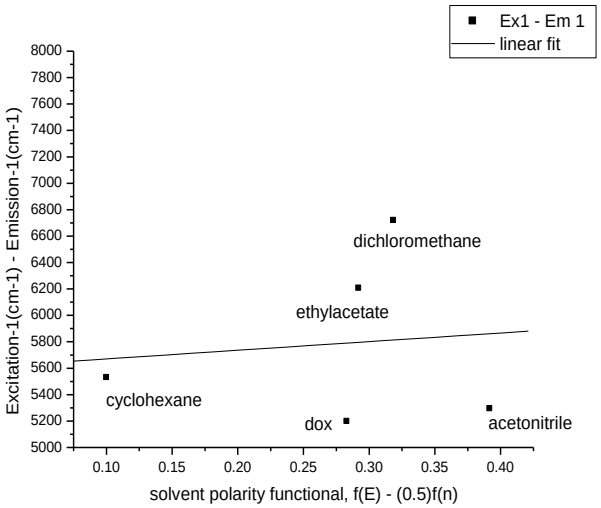

Fig. 35 Plot of Stokes shift of 1st excitation and emission (LE) state vs. solvent polarity function

As shown in the figure, the slope of the plot of Stokes shift for the first excitation and first emission is found to be 653 cm^{-1}. Application of Lippert plots and taking the Onasgar cavity radius as the radius of the molecule (DMABA-Amtr), 5Å, the dipole moment change becomes only 2.85 D as predicted for the LE emission. On the other hand the plot of Stokes shift for the second excitation and second emission is presented in Fig.36.

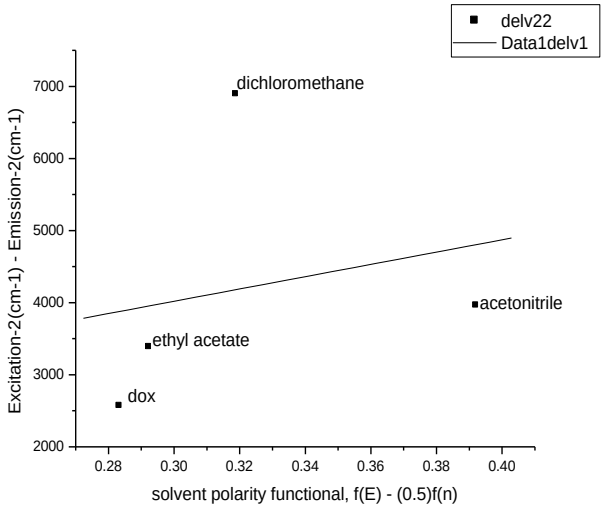

Fig.36 Plot of Stokes shift of the second excitation and emission (LE state) versus solvent polarity function.

From the figure, the plot of Stokes shift for the second excitation and second emission is found to be 8520 cm^{-1}, which is significantly different from the first Stokes shift. Similar application of the Lippert-Mataga equation for the second Stokes shift gives a dipole moment change (between the ground state and the excited state) value of 10.3 D.

Thus, from the plots above, it can be shown that the second excitation spectrum is more shifted to the red-side than the first one. This indicates a greater dipole moment for the second species (the one excited at longer wavelength) than the first one (the one excited at shorter wavelength). The fluorescence spectra show large Solvatochromic shift for the CT fluorescence indicating a high degree of charge transfer for the emitting state.

From computational results (at DFT/B3LYP/6-31G level), the ground state dipole moment for the optimized geometry is found to be 8.8507 D. Assuming the ground state dipole moment of the two conformers to be the same for simplicity, it follows that μ_{e1} = 11.7 D, and μ_{e2}

= 19.2 D. The results presented so far strongly supports the hypothesis of the existence of the equilibrium between two species formed in the ground state and which both fluoresce when they are excited. It was found out that the property of the emission spectrum is strongly dependent on the wavelength of the exciting light. This dependency of emission spectrum on the wavelength of the exciting light and the presence of an isoemissive point can only be explained by the presence of two relatively stable systems in equilibrium. Therefore, this fact together with the existence of two excitation bands indicates that DMABA-Amtr has two stable conformers in the ground state, which are in equilibrium.

6. Computational Results

During the assessment of the potential energy surface (PES) of the compound, the reaction coordinate is defined as the tortional angle between the plane of dimethyl amino group and that of the benzene ring (Schem III). The energy of the ground electronic state increases along the twisting coordinate and the result predicts two minimum structure of the compound in vacous (Fig.30).

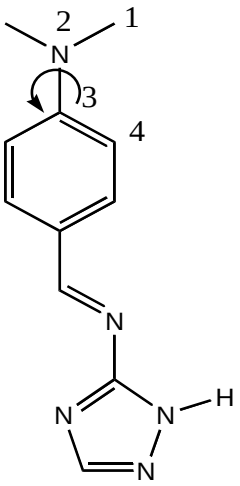

Scheme III: The axis of rotation used for the computational work.

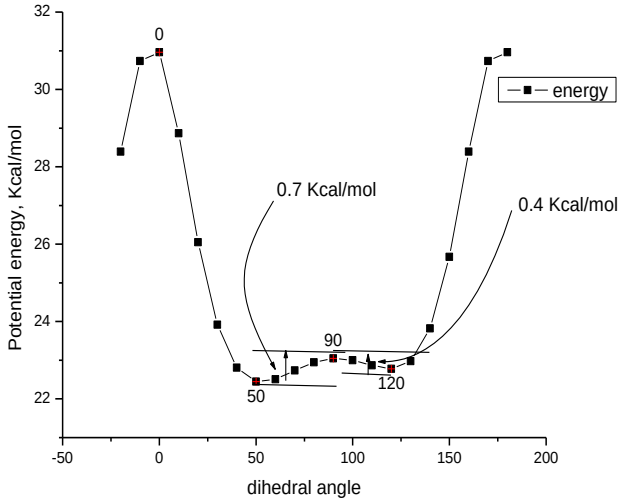

Fig.37 Potential energy surface (PES) of DMABA-Amtr in vacuum.

In Fig.37, the potential energy surface of DMABA-Amtr in vacous shows two mimimum structures at 50^0 (conformer A)and 120^0 (Conformer B). The energy of activation to interchange one another is calculated to be 0.7 and 0 .4 kcal mol^{-1} for conformer A and B, respectively. The energy barriers for both conformers are less than the available room temperature thermal energy, $3/2RT = 0.9\,\text{Kcal mol}^{-1}$. This indicates that room temperature thermal energy is enough to exchange one conformer in to the other. Hence the equilibrium structure of the molecule in vacuum is coming from the contribution of the two conformers and it will appear as a single ground state species.

The situation, however, becomes completely different in polar solution. The potential energy surface of DMABA-Amtr in water (polar environment) is shown in Fig.38.

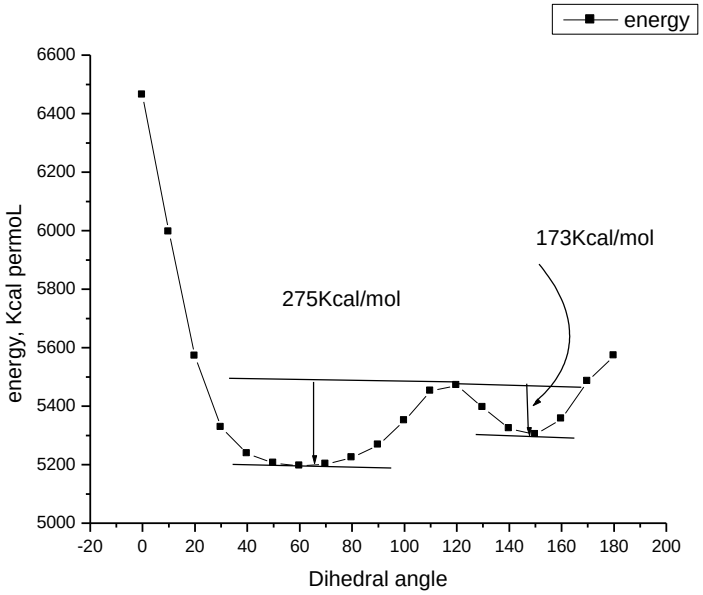

Fig.38 Potential energy surface (PES) of DMABA-Amtr in water (Polar environment).

As shown in the figure, the potential energy surface of DMABA-Amtr in polar environment shows two minimum structures at 60^0 (conformer A) and 150^0 (Conformer B). The energy of activation to interchange the conformers one another is calculated to be 275 and 173 kcal/mol for conformer A and B, respectively. The energy barriers for both conformers are much higher than the available room temperature thermal energy, $3/2RT = 0.9\,\text{Kcal mol}^{-1}$. This indicates that the two conformers can exist in polar solvents independently and hence gives independent

photophysical characteristics (such as independent excitation and emission spectra).

Thus, comparison of the present experimental and theoretical studies on DMABA-Amtr indicates that the dual emission observed is likely to originate from two different conformations (nearly planar and tilted) of DMABA-Amtr at equilibrium. These conformers A and B can be assigned to the short wavelength emitting and long wavelength emitting species, respectively.

From the experimental and theoretical studies so far, we propose the following two structures for the conformers (A) and (B) of DMABA-Amtr (Schem IV)

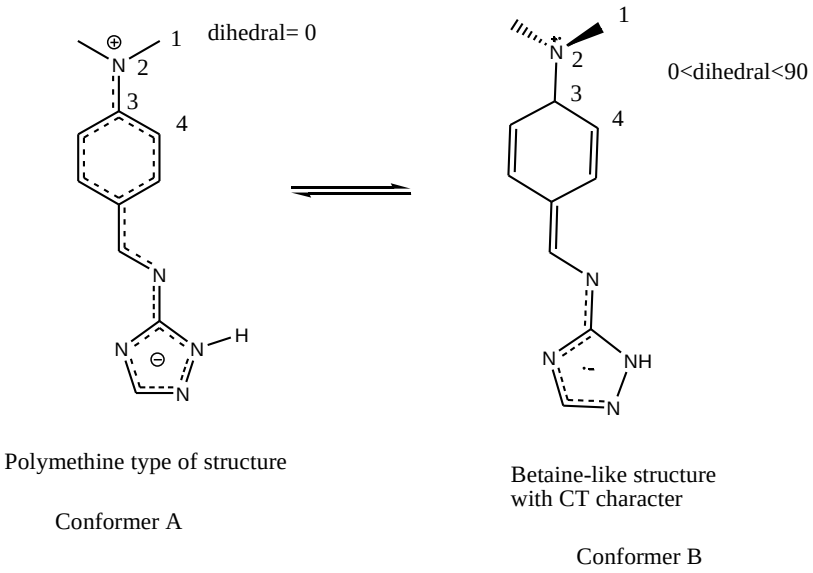

Scheme IV: Proposed structures that may exist in equilibrium.

From the figures above, it can be seen that conformer A has polymethine-like structure in which both the donor and acceptor groups containing nitrogen. In this case since the electron donating and accepting capacity of the groups is comparable, the change in the dipole moment during electronic transition is expected to be lower and this is actually the case found in which there is a small dipole moment change between the ground and excited state (only 2.85 D). however for the second conformer involving greater charge transfer (due to the tilted conformation of the dimethylamino moiety and hence partial decoupling, that prevent back donation from the triazole moiety), a larger change in dipole moment (10.3 D) is found. And this partial charge transfer in conformer B can be the reason for the larger solvatochromic shift observed in the excitation and emission spectra of conformer B.

According to the previous models, for example, TICT model, the basis of dual fluorescence is the 90^0 twist of the donor group and thereby complete decoupling of the donor and acceptor orbitals leading to full charge transfer (schem V). This full charge transfer has been attributed to be responsible for the long wavelength emission band. So possibility of full charge transfer in DMABA-Amtr is computed by applying the definition of dipole moment, $\mu = er$,

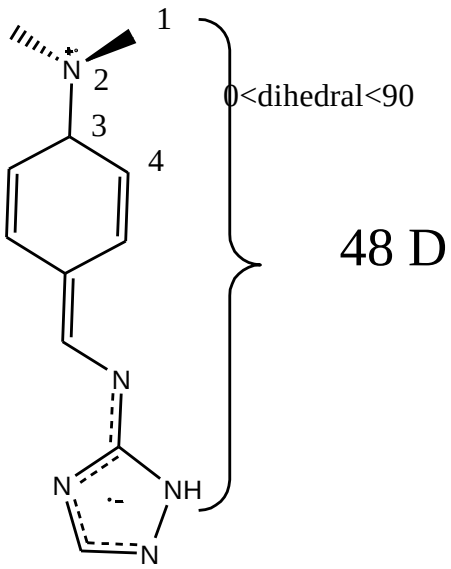

Scheme V: Theoretically computed dipole moment for the so called TICT state.

The value found experimentally, 19.2 D is less than the calculated value, even taking part of the negative charge center possible of resonating to farther distance, 48 D. So it is only possible to say that there is a charge transfer, which causes the second long wavelength emission and there is no full charge transfer. Hence orbital decoupling does not occur. Hence the TICT model cannot account for the dual emission in DMABA-Amtr. From the results it can be shown that the effective charge transfer is only 39.6 % and the effective charge transfer length is 40%.

Since the PICT mechanism also assumes dual emission from two species in the excited state, the experimental results clearly showed that this is not the case.

7. Conclusion

In this paper we have examined the excitation wavelength dependency of the emission spectra of DMABA-Amtr in polar solutions using steady-state fluorescence spectroscopy. The ultimate goal is to show that the ground state of DMABA-Amtr consists of two conformational isomers of the molecule.

A closer examination of the excitation spectra of DMABA-Amtr in polar solvents showed two characteristic independent excitation bands. Also examination of its emission spectra showed that the spectrum consists two emission bands with the LE to CT intensity ratio dependent on the wavelength of the exciting light. These observations suggest that the compound, in its ground state, exists in the form of two relatively stable conformers, which are in equilibrium.

As the wavelength of excitation increases, there is a change in band form in the emission spectrum. This shows that one can selectively excite one of the spectral features of the dual fluorescence. After selective excitation, the intensity of the bands is proportional to the excitation wavelength, while the band form remained the same, indicating the presence of two separate absorption bands in the ground state of DMABA-Amtr.

On the basis of the experimental results and PES diagrams, we suggest that there are two conformers of DMABA-Amtr, which are stable in the ground state, equilibrated in solution at room temperature that give rise dual fluorescence upon excitation.

8. References

[1] R.B. Singh, S. Mahanta, S. Kar and N. Guchhait, J. Lumin. 128 **(2008)** 1421-1430.

[2] N. Dash, F.A.S. Chipem, R. Swaminathan and G. Krishnamoorthy, Chem. Phys. 460 **(2008)** 119-124.

[3] Z.R. Grobawski, Pure & Appl. Chem. Vol. 65, No.8, **(1993)**, 1751-1756.

[4] S. Sumalekshmy and K.R. Gopidas, J. Phys. Chem. B, 108, **(2004)**, 3705-3712.

[5] R.B. Singh, S.Mahanta, S Kar and N. Guchhait, Chem Phys. 342 **,(2007)**, 33-42.

[6] A. Kawski, B. Kuklinski and P. Bojarski, Chem. Phys. 455, **(2008)**, 52-54.

[7] R. Daum, S. Druzhinin, D. Earnst, L. Rupp, J.Schroeder, K.A. Zachariasse, Chem. Phys. Letters, 341 **(2001)**, 272-278

[8] M.Balon, C. Carmona, M.A. Munoz, Chem. Phys. 302, **(2004)**.

[9] C. Yao, H. B. Kraatz, R. Steer, Photochem. Photobiol.Sci, 4, **(2005)**, 191-199

[10] P. Purkayastha, N. Chattopadhyay, Phys. Chem. Chem. Phys, 2, **(2000)**, 203-210

[11] A.M.J. Campana, F.A. Barrero, M.R. Ceba, Analyst, **(1992)**, 117

[12] M. Kagayama, Y. Sasano, H. Satos, S. Kamakura, K. Motegi, I.M. Izoguchi, J. Anathomy and Embryology, **(2004)**, 233-238

[13] A. Polimeno, A. Barbon, P.L. Nordio, J.Phys. Chem. **(1998)**, 12158-12168

[14] A. Maliakal, G. Lem, N.J. Turro, R. Ravichandran, J.C. Suhadolink, A.D. Debellis, M.G. Wood, J. Lau, J.Phys. Chem. A **(2004)**, 106, 2002, 7680-7689

[15] I. Szydlowska, A. Kyrychenko, A. Gorski, J. Waluk, J. Herbich, Photochem. Photobiol.Sci, 2, **(2003)**, 187-194

[16] J. Dobkowski, W. Retting, J. Waluk, Phys. Chem. Chem. Phys, 4, **(2002)**, 4334-4339

[17] R.B. Singh, S. Mahanta, S. Kar and N. Guchhait, J. Lumin. 128 **(2008)** 1421-1430.

[18] T. Pal, M. Paul and S. Ghosh, J. Mol. Struct. (THEOCHEM) 860 **(2008)** 8-12

[19] J. D. Walson, Prac. Nat. Acad. Sci, USA, 69, 9**, (1972)**, 2488-2491

[20] S. Maheshwari, A. Chowdhury, N. Sathyamurthy, M. Panda, J. Chandrasekhar, J.Phys. Chem. A,103, **(1999)**, 6257-6262

[21] T.L. Arbeloa, F.L. Arbeloa, M.J. Tapia, I.L. Arbeloa, J.Phys. Chem. 97, **(1993)**, 4704-4707

[22] Z.R. Grabowski, Pure & Applied Chem, 65, 8, **(1993)**, 1751-1756

[23] F. Pine, M.J. Melo, H. Santos, J.C. Lima, I. Abreu, R. Ballardini, M. Maestri, New J. Chem., **(1998)**, 1093-1098

[24] C. Richardit, Solvent and Solvent effect in organic chemistry, 3rd edition, WILLEY-VCH, Weinheim, **(2003)**, 329-387.

[25] Dobkowski J., Wojcik J., Kozminski W., Kols R., Waluk J., Michl J.; J. Am. Chem. Soc. **(2002)**, 124, 2406.

[26] Yoshihara T., Druzhinin S. I., Zachariasse K., J. Am. Chem. Soc. **(2004)**, 126, 8535.

[27] Okamoto H., Inishi H., Nakamura Y., Kohtani S., Nakagaki R., J. Phys. Chem. A, 105, **(2001)**, 4182-4188.

[28] Kowk W. M., Matousek P., Parker A. W., Phillips D., Toner W. T., Towrie M., Umapathy S., J. Phys. Chem. A, 105, **(2001)**, 984-990.

[29] Dreyer J., Kummrow A. J. Am. Chem. Soc.122, **(2000)**, 2577-2585.

[30] Zilberg, S.; Haas, Y. J. Phys. Chem. A, 106, **(2002)**, 1-11.

[31] Rappoport, D.; Furche, F. J. Am. Chem. Soc, 126, **(2004)**, 1277-1284.

[32] Köhn, A.; Hättig, C. J. Am. Chem. Soc. , 126, **(2004)**, 7399-7410.

[33] Serrano-Andrés, L.; Merchán, M.; Roos, B. O.; Lindh, R. J. Am. Chem. Soc ,117, **(1995)**, 3189-3204.

[34] Sobolewski, A. L.; Sudholt, W.; Domcke, W. J. Phys. Chem. A, 102, **(1998)**, 2716-2722.

[35] Parusel, A. B. J.; Köhler, G.; Grimme, S. J. Phys. Chem. A, 102, **(1998)**, 6297-6306.

[36] Parusel, A. B. J.; Köhler, G.; Nooijen, M. J. Phys. Chem. A,103, **(1999)**, 4056-4064.

[37] Kim, H. J.; Hynes, J. T. J. Photochem. Photobiol., A: Chem, 105, **(1997)**, 337-343.

[38] Mennucci, B.; Toniolo, A.; Tomasi, J. J. Am. Chem. Soc, 122, **(2000)**, 10621-10630.

[39] Semyon Cogan, Shmuel Zilberg, and Yehuda Haas, J. Am. Chem. Soc , 128, **(2006)**, 3335-3345.

[40] M. Barzoukas, C. Runser, A. Fort, M. Blanchard-Desce, Chem. Phys. Letters , 257, **(1996)**, 531-537.

[41] F. Wurthner, S.Yao, J. Schilling, R. Wortmann, M. Redi-Abshiro, E. Mecher, F. Gallego-Gomez, K. Meerhlz, J. Am. Chem. Soc , 123, **(2001)**, 2810-2824.

[42] A.Yu, Catherine A., D.A. Farrow, D.M Jonas, Phys. Chem. A 106, **(2002)**, 9407-9419

[43] Frank Jensen, Introduction to computational chemistry, WILEY, **(2004)**.

[44] B. Valeur, Molecular fluorescence: Principle and Application, Wiley-VCH Verlag FmbH **(2001)**.